Chemical Science International Journal
18(1): 1-34, 2017; Article no.CSIJ.28976
Previously known as American Chemical Science Journal
ISSN: 2249-0205

SCIENCEDOMAIN *international*
www.sciencedomain.org

Evaluation of Performance of Corrosion Inhibitors Using Adsorption Isotherm Models: An Overview

Ekemini Ituen[1*], Onyewuchi Akaranta[1,2] and Abosede James[2]

[1]African Centre of Excellence in Oilfield Chemicals Research, Institute of Petroleum Studies, University of Port Harcourt, Nigeria.
[2]Department of Pure and Industrial Chemistry, University of Port Harcourt, Nigeria.

Authors' contributions

This work was carried out in collaboration between all authors. Author EI designed the study, managed the literature searches and wrote the first draft of the manuscript. Authors OA and AJ supervised the review process. All authors read and approved the final manuscript.

Article Information

DOI: 10.9734/CSJI/2017/28976
Editor(s):
(1) Georgiy B. Shul'pin, Semenov Institute of Chemical Physics, Russian Academy of Sciences, Moscow, Russia.
Reviewers:
(1) S. Srinivasa Rao, V. R. Siddhartha Engineering College, Vijayawada, Andhra Pradesh, India.
(2) Innocent Hapaari, National University of Lesotho, Lesotho.
(3) Wu-Jang Huang, National Pingtung University of Science and Technology, Taiwan.
(4) Hai-Yin Yu, Anhui Normal University, China.
Complete Peer review History: http://www.sciencedomain.org/review-history/17611

Review Article

Received 16th August 2016
Accepted 2nd September 2016
Published 26th January 2017

ABSTRACT

Adsorption isotherm models are an important tool for describing interaction of corrosion inhibitors with metal surfaces which they are aimed to protect. In this paper, key adsorption isotherms used in corrosion inhibition studies have been reviewed. We have examined how some deductions on the nature of metal-corrosion inhibitor interactions are obtained from certain parameters and interpreted to characterize the adsorption of the corrosion inhibitors and their mechanisms of inhibition. More attention is paid to their applications and the useful information that may be derived from them than on their background and derivation. Efforts have also been made to identify some limitations (where applicable) and/or discrepancies in usage of some models in reporting experimental findings. Informed by some inconsistencies observed from some literature reports, critical suggestions on appropriate approaches to collection and processing of data for fitting into these isotherms have been made. This paper will be a beneficial secondary source of information to readers and invaluable reference material to experts and future researchers in the subject area.

**Corresponding author: E-mail: ebituen@gmail.com;*

Keywords: Active site; adsorption isotherm; corrosion inhibitor; equilibrium constant; molecular interaction parameter; monolayer; size parameter.

1. INTRODUCTION

When metals come in close contact with aggressive media, their surfaces corrode. The speed and extent of the corrosion process depends on several factors like concentration of the aggressive medium and temperature. Corrosion inhibitors have been employed extensively to control corrosion of metals in various aggressive media. It is generally believed that a given corrosion inhibitor functions by adsorption on metal surface and formation of thin protective film(s) or layer(s) that 'blanket(s)' the metal surface from the aggressive medium. The nature of interaction between the film formed and the metal surface may be explained with the help of adsorption isotherms. This involves the use of appropriate plots to determine some parameters (depending on the model) that provide some useful information for predicting what happens at the adsorbed layer. Adsorption involves adhesion (or concentration) of atoms, molecules or ions on the surface of a substance, most often, a solid. The surface to which the molecule or atom is adhering is called the adsorbent while the molecule or atom itself is called the adsorbate. Therefore, the adsorption phenomenon is essentially an attraction of adsorbate species on the adsorbent surface. The preferential concentration of adsorbate molecules in the proximity of the adsorbent surface arises from the unsaturated nature of surface forces of the adsorbent. Verma et al. [1] opines that adsorption of corrosion inhibitors may be seen as a substitution process where the inhibitor molecules in the aqueous phase replace water molecules already adsorbed on metal surface.

Most often, two of the three phases of matter can come in contact with one another, leaving a boundary between them called interface. Several important biological, chemical and physical phenomena take place at interfaces [2], one of which is adsorption. Most practical interfaces that support the adsorption phenomenon are solid-gas and solid-liquid. In both cases, the solid is the adsorbent while the adsorbate is liquid or gas. Many technical methods, industrial applications and experimental principles are founded on application of adsorption phenomena. Examples include precipitation, chromatographic separations, electrochemical techniques, coagulation-flocculation, some biological processes, membrane processes, filtration, catalysis, sedimentation, waste water treatments, removal of pollutants from aqueous and gaseous environments, floatation, chemical reactions, etc. [3-20]. Data obtained from some of such experiments may be fitted into adsorption isotherms for further explanations. Adsorption phenomenon is simple, economically viable, experimentally feasible, industrially applicable and scientifically acceptable, which may account for its extensive application [17]. Though practical application of effective adsorbents and adsorbates was limited initially by high cost, toxicity and difficulties of regeneration, growing research has opened doors to low low-cost, renewable and environmentally friendly materials such as plant biomasses used in corrosion inhibition, water treatment, decontamination and remediation processes [21,22].

The mechanism by which adsorption takes place may be physical or chemical in nature, also referred to as physisorption or chemisorption respectively. Physical adsorption is associated with weak van der Waals or electrostatic interactions between the adsorbent and the adsorbate in the neutral or ionic form respectively. However, when the adsorption of one or several ionic species is accompanied by simultaneous desorption of an equivalent ionic species, the phenomenon is considered as ion exchange [2]. Physical adsorption may also be viewed as a condensation process in which the adsorbate condenses on the surface of the adsorbent. This makes physisorption reversible since the molecules may evaporate from the surface under certain conditions, a process known as desorption. Physisorption occurs at temperatures lower or close to the critical temperature of the adsorbate and may involve formation of multi-molecular layers of adsorbate on the adsorbent. Opposed to physisorption, chemical adsorption mechanism involves the formation of a monolayer of the adsorbate and occurs at temperatures much higher than the critical temperature of the adsorbate. Actual chemical bonds may be formed which makes chemisorption irreversible. Fortunately, both processes are often exothermic and may occur simultaneously under suitable conditions.

To predict whether an adsorption process is physical or chemical in nature, a correlation between the degree of responsiveness of amount of adsorbate condensed on the surface at a given condition and changes in some critical

factors such as concentration, pressure or time is evaluated. These correlations are represented in lines or curves called adsorption isotherms. A typical illustration of adsorption isotherm is shown in Fig. 1. Notwithstanding the model used to obtain the isotherm, a component of the isotherm usually involves a function of the degree of surface coverage (also called fractional coverage) described as amount of the adsorbate taken up by the adsorbent surface to the initial amount present.

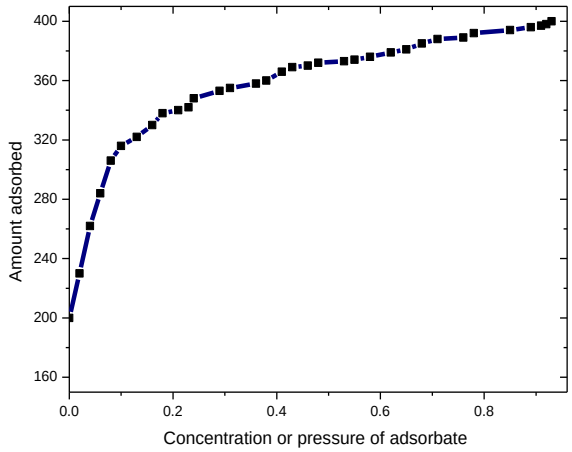

Fig. 1. Schematic representation of an adsorption isotherm

Various adsorption isotherms models have been derived and used to describe different adsorption processes and mechanisms. Details on derivation of these isotherms and how the adsorbates are held on the adsorbent surface are available in the literature [17,18,23]. The present study examines the isotherms that have been used to explain interaction of corrosion inhibitors on metal surfaces. A brief supporting background of the graphical implication of the models and some limitations (where applicable) at certain conditions have also been described. Some discrepancies observed in interpretation of the associated parameters in some reports are identified. Readers, current and future researchers in the field will find this paper a useful secondary source of information and/or reference material since it also covers as much as possible, the basis of the subject matter.

2. ADSORPTION ISOTHERMS

Consider the schemes in Fig. 2 where the adsorbate constitutes the bulk phase and is in contact with the surface of the adsorbent. If the adsorbate and adsorbent are contacted for long enough, equilibrium may be established between the amounts of inhibitor molecules adsorbed and that amount remaining in the bulk phase. The equilibrium relationship is easily described using adsorption isotherm - a plot that relates the amount of adsorbate adsorbed to the equilibrium concentration of the inhibitor at a given temperature. This amount adsorbed (θ) is expressed as a function of inhibitor concentration (*C*) in the bulk medium and may be represented by the general form [24]:

$$f(\theta, x)e^{(-2a\theta)} = KC \quad (1)$$

where $f(\theta, x)$ represents the configuration factor which depends on the physical model and assumptions underlying the derivation of the particular model. K is the adsorption equilibrium constant which describes how strongly the molecules are held on the adsorbent surface and *a* is the molecular interaction parameter used to predict the nature of interactions in the adsorbed layer. Most adsorption isotherms used for study of corrosion inhibitors are derived from this general form and amended to fit certain purpose(s) and assumptions.

2.1 Adsorption of Corrosion Inhibitors

In corrosion studies, it is presumed that the corrosion inhibitor functions by initial diffusion from bulk medium to the metal surface and subsequent adsorption on the surface. Little effort has been made in understanding the manner and speed of diffusion of these inhibitor molecules so far, but our research group is currently working on some theoretical diffusion models that may sufficiently describe this phenomenon. However, the mechanism of adsorption is understood and has been a very active field of research. Four forms of adsorptive interactions that may take place at the metal-inhibitor interface are [25,26]:

- electrostatic interaction between charged metal surface and charged inhibitor molecules;
- interaction of uncharged electron pair (which may come from non-bonding orbitals of hetero atoms) of the inhibitor molecules with the metal;
- interaction of pie-electrons with the metals; or
- a combination of two or more of the above.

The first case exemplifies physical adsorption mechanism; the next two are associated with chemical adsorption mechanism; and the last with mixed or physio-chemisorptions.

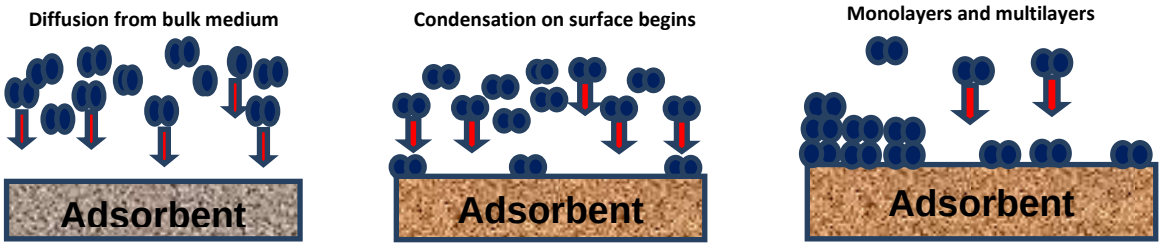

Fig. 2. Schematic representation of adsorption of molecules on solid surfaces from bulk phase

2.2 Variables for Construction of Adsorption Isotherms

The chemical dissolution of metal (e.g. iron) in acid (e.g HCl or H_2SO_4) may be illustrated as follows:

$$Fe_{(s)} + 2HCl_{(aq)} \rightarrow FeCl_{2(aq)} + H_{2(g)} \quad (2)$$

$$Fe_{(s)} + H_2SO_{4(aq)} \rightarrow FeSO_4 + H_{2(g)} \quad (3)$$

and may be monitored by [27]:

- determining the mass of $Fe_{(s)}$ left (or lost) after dissolution at a given time frame by weight loss technique;
- determining the changes in activity or electrochemical potential of the solution by electrochemical measurements;
- measuring the volume of hydrogen gas evolved with time by gasometric technique;
- determining the amount of the $Fe_{(s)}$ leached into the solution at intervals by atomic absorption spectroscopy (AAS), and so on.

The simplest, convenient and most widely used technique for monitoring corrosion of metal samples and their inhibition is the gravimetric (weight loss) technique [28-47]. Papavinasam et al. [48] claimed that weight loss measurement combined with characterization of pits gives the most reliable technique for monitoring metal corrosion. At least three repeated measurements could be made for the same test and standard deviation calculated such that the data presented would be at least within 95% confidence interval [49] while outliers could be discarded according to Grubbs statistical test [50]. Weight loss method is also useful because it provides a direct means of evaluating the degree of surface coverage from corrosion rate or inhibition efficiency (Eq. 4-6). Usually, a pre-weighed metal coupon is immersed in a test solution (usually simulated using acid with and without the corrosion inhibitor) for a chosen time interval, *t*. It is then retrieved, cleaned and re-weighed. Assuming the initial and final weights of the coupons are w_1 and w_2 respectively, corrosion rate (*R*), percentage inhibitor effectiveness (inhibition efficiency), $\mathcal{E}_{inh}$, and dimensionless degree of surface coverage (θ) can be calculated as follows:

$$R = \frac{w_1 - w_2}{At} \quad (4)$$

$$\mathcal{E}_{inh}, = 100\left(\frac{R_b - R_i}{R_b}\right) \quad (5)$$

$$\theta = 0.01\mathcal{E}_{inh} \quad (6)$$

where R_b and R_i are the corrosion rates in the absence and presence of the inhibitor and A is the surface area of the metal specimens.

The electrochemical technique has also been employed extensively for this purpose [51-62]. The technique involves measurement of resistance or current using an electrochemical workstation. Details on how to obtain the associated variables have been explained earlier [30,33]. Inhibition efficiency can be calculated from any of polarization resistance (Eq. 7), charge transfer resistance (Eq. 8) or corrosion current density (Eq. 9).

$$\theta = 0.01\left(\frac{r_i - r_b}{r_i}\right) \quad (7)$$

$$\theta = 0.01\left(\frac{r_{CTI} - r_{CTB}}{r_{CTI}}\right) \quad (8)$$

$$\theta = 0.01(1 - {}^{I_i}/_{I_b}) \quad (9)$$

where r_b and r_i are the polarization resistance in the absence and presence of the inhibitor respectively, r_{CTB} and r_{CTI} are the charge transfer resistance in the absence and presence of inhibitor respectively and I_b and I_i are the corrosion current density in the absence and presence of the inhibitor.

The last two of the four methods above may be considered less efficient because they do not

always provide true measurement of the corrosion rate. The use of hydrogen evolution technique is still being developed and recently has been improved to study real-time kinetics for hydrogen energy supply source by corrosion of soft metals [63-74]. Use of AAS appears to be going to extinction although there are some reports in literature [75-77]. Thermometric measurement and other methods have also been used but the data obtained are sometimes not comparable with those of weight loss and electrochemical techniques. The baseline for these measurements is the corrosion rate and inhibition efficiency data which are used to compute the degree of surface coverage which is the principal parameter for fitting into adsorption isotherm models [78-80].

2.3 Adsorption Isotherms Models Employed in Corrosion Inhibition Studies

Although there are many adsorption isotherms for interpreting various research findings [23, 81], some of them are not amendable for use for adsorption of corrosion inhibitors. The models proposed by Langmuir, Temkin, Flory-Huggins, Frumkin, Freundlich and the so-called thermodynamic/kinetic (El-Awady et al.) isotherms are often applied to corrosion inhibitors. In each case, a function of the fractional surface coverage (θ) is plotted against a function of the concentration of inhibitor (C) and the associated adsorption parameters are deduced from slope or intercept or both. Thermodynamic functions which define the nature of the inhibitor-metal interaction can also be obtained from some of these parameters.

2.3.1 The Langmuir adsorption isotherm

As far as adsorption of corrosion inhibitors on metal surfaces is concerned, Langmuir adsorption isotherm model is the most extensively used. Irving Langmuir in 1916 developed this model to explain the relationship between surface coverage of an adsorbed gas and the pressure of the gas over the surface of its adsorbent at constant pressure. He assumed a monolayer adsorption of the adsorbate at fixed number of definite localized adsorption sites. The molecules were assumed to be identical and equivalent with no lateral interaction or steric hindrance between them. All the sites on the adsorbent were also assumed to possess equal affinity for the adsorbate, and possess constant sorption activation energy and enthalpy [82, 83].

The surface coverage and pressure (*P*) of the gas relates as shown in Eq. 10 below:

$$P = K\left(\frac{\theta}{1-\theta}\right) \tag{10}$$

where K is the equilibrium constant for the adsorption-desorption process. The adsorption process may be seen as condensation while desorption as evaporation of the adsorbate molecules with respect to the surface.

The above model (Eq. 10) appears to present the adsorption-desorption concept from the equilibrium point of view. To apply this model for corrosion inhibitors, the gas molecules are replaced with corrosion inhibitor molecules and the metal surface becomes the adsorbent. Equilibrium becomes a state where the rate of adsorption of the inhibitor molecules on the metal surface is exactly opposed by the rate of desorption of the same molecules back into the bulk solution. It will be convenient to monitor a more practically measureable property of an aqueous phase like concentration (*C*) than pressure, since pressure is also function of concentration and temperature (T), i.e.

$$P = f(C,T) \tag{11}$$

If we 'invoke' Eq. 11 into Eq. 10, we obtain Eq. 12 below and the parameters can be obtained from corrosion experiments:

$$C\left(\frac{1-\theta}{\theta}\right) = K^*(T) \tag{12}$$

where $K^*(T)$ is a temperature dependent constant, contains an experimental term of the form [….. $e^{(-\frac{\Delta H_{ads}}{RT})}$] and is reciprocal to the equilibrium constant of adsorption-desorption process ($K_{ads} = 1/K^*$). The value of K_{ads} obtained from the reciprocal of the intercept on the ordinate of the Langmuir isotherm should decrease with increase in temperature and strength of adsorption.

In practice, the Eq. 12 is linearized to obtain Eq. 13 or 14 and linear plots made as shown in (a) and (b) in Fig. 3 respectively using values reported earlier for inhibition of mild steel corrosion in 2 M HCl by different concentrations of 5-HTP at different temperatures [27].

$$\frac{C}{\theta} = 1/K_{ads} + C \tag{13}$$

$$\log(\frac{\theta}{1-\theta}) = \log C + \log K_{ads} \tag{14}$$

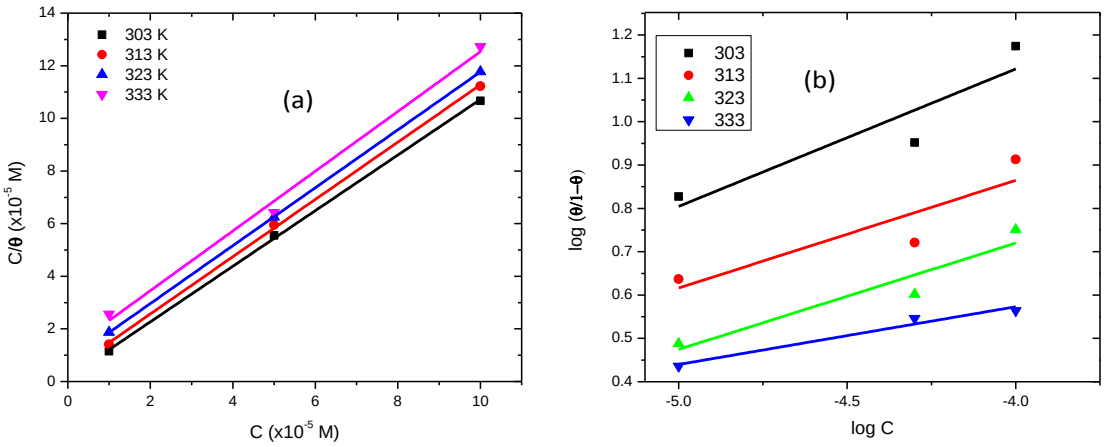

Fig. 3. Langmuir adsorption isotherms for inhibition of mild steel corrosion in 2.0 M HCl by different concentrations of 5-HTP at temperatures 303 K to 333 K [27]

For the adsorption of a given inhibitor to show maximum adherence to the Langmuir model and the assumptions upon which it was derived, the slope of the plot should be unity. Particularly important to the corrosion scientist is whether the adsorbed film formed involves a monolayer or multilayer and whether there are interactions in the adsorbed layer. It is believed that the closer the slope is to unity, the more likely the inhibitor obeys the Langmuirian model, within limits of systematic or experimental error. Sometimes, the slope obtained may deviate markedly from unity, implying that the adsorption is not monolayer and Langmuir model cannot be used to describe the inhibitor adsorption. Hybrid isotherms may be used as a way out, namely, the so-called modified Langmuir (or Villamil) adsorption isotherm or the Langmuir-Freundlich isotherm [37,84,85].

2.3.2 The modified Langmuir adsorption isotherm

Shaban et al. [52] claimed that a slope greater than unity obtained from Langmuir isotherm could signify that one or more of each inhibitor unit occupies more than one adsorption site; there are interactions between adsorbed species on the metal surface; or the adsorption heat (enthalpy) changes with increasing surface coverage. These were factors not taken into consideration in the derivation of Langmuir isotherm. A compensation factor 'n' was introduced into the conventional Langmuir equation so that Eq. 13 becomes:

$$C/\theta = nC + n/K_{ads} \quad (15)$$

The factor 'n' is obtained from the slope and represents the number of displaced water molecules initially adsorbed on the metal surface. Consequently, 'n' can be used to predict the number of molecules of the inhibitor adsorbed per active site of the metal surface. Using values reported for 5-HTP, this model yields linear plots similar to that shown in Fig. 4.

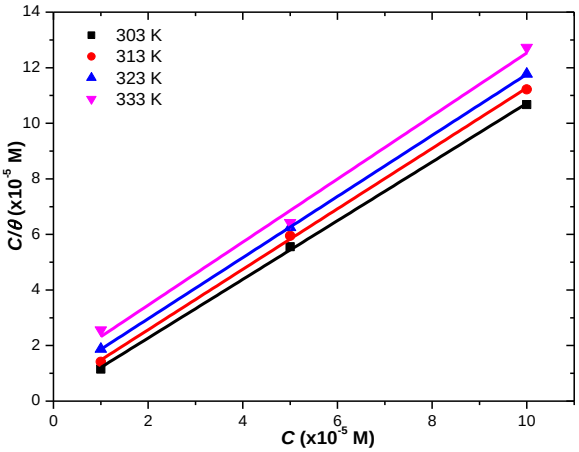

Fig. 4. Modified Langmuir adsorption isotherm for inhibition of mild steel corrosion in 2.0 M HCl by different concentrations of 5-HTP at temperatures 303 K to 333 K [27]

Critical reasoning may quickly reveal that where more than a molecule is adsorbed at a particular active site of a metal (as allowed by this assumption), a probability function describing the mode of binding per molecule could arise. Such probability function may be similar to or different from the binding kinetics of enzymes or catalysts on their substrates, which may be sequential or concerted. A survey of literature however reveals

that adsorption of corrosion inhibitors has not been explained using this approach, a gap our research group also aims to explore in future studies by finding models that can be used to explain this binding probability. Our findings will be reported in due course. For the purpose of this paper, concentration is on adsorption isotherm models. A likely set-back of the modified Langmuir model is its failure to provide information on whether there is/are or not interaction(s) between surface adsorbed species and the nature of the adsorption.

2.3.3 The Langmuir-Freundlich adsorption isotherm

This model (Eq.16) has been used to describe multi-site adsorption behavior of corrosion inhibitors on heterogeneous surfaces without considering interactions among the inhibitor molecules [85]. The term '*K'* represents the usual adsorption equilibrium constant while x represents the heterogeneous parameter.

$$\theta = \left(\frac{(KC)^x}{1+(KC)^x}\right) \quad (16)$$

Tian et al. reported that the values of x lie within 0 and 1, inclusive, and is associated with the distribution of adsorption energy at the different sites on a non-ideal surface [85]. To understand this, we assume an initial heterogeneous surface with each site having different adsorption energies and different affinities for inhibitor molecules. If $x = 1$, the model becomes Langmuirian and can no longer describe non-ideal situations. Furthermore, as the value tends to unity $(x \rightarrow 1)$, the adsorption energy difference between the sites becomes narrower and the sites seem to become equivalent and homogeneous with very close range of distribution of adsorption energy. It is also reflecting a situation proximate to the Langmuirian. Therefore, for this model to suitably describe heterogeneous systems, values of x should be as farther away from unity as possible. Interestingly, when the value is zero or tends to zero, the inhibitor should be expected to be approximately theoretically 50% efficient. This model is not commonly applied to corrosion inhibitors perhaps due to uncertainty that may be associated with assigning value to x. A plausible observation from this model is that it may be possible to theoretically estimate the concentration of the inhibitor that will give an inhibition efficiency of 50% by setting x = 0, but this remains an observation until further empirical data validates it.

2.3.4 Temkin adsorption isotherm model

Another familiar adsorption isotherm which has also been extensively employed in the description of mechanism of action of corrosion inhibitors is the Temkin model. Unlike others discussed so far, it provides some insights on the nature of interactions taking place in the adsorbed layer. The model is expressed as follows:

$$e^{-2a\theta} = KC \quad (17)$$

where a is the molecular interaction parameter. Molecular interaction parameter, depending on its sign, is used to predict whether attraction or repulsion takes place in the adsorbed layer. The linearized form of the equation (Eq. 18) can be used to obtain linear plots of θ against $\ln C$ (Fig. 5).

$$\theta = -\frac{1}{2a}\ln C - \frac{1}{2a}\ln K \quad (18)$$

The value of K describes how strongly the inhibitor molecules are adsorbed on the metal surface.

2.3.5 The Freundlich adsorption isotherm model

This model is expressed in the equation:

$$\theta = KC^{1/n} \quad (19)$$

where n is an empirical constant. The linearized form of the model (Eq. 20) is preferred for plotting isotherms (see Fig. 6). A linear plot of log θ against log *C* is obtained.

$$\log\theta = \log K + \frac{1}{n}\log C \quad (20)$$

The value of $\frac{1}{n}$ is used to describe the ease of adsorption. Usually, when $0 < \frac{1}{n} < 1$, adsorption is believed to be easy, and moderate or difficult when $\frac{1}{n} = 1$ or $\frac{1}{n} > 1$ respectively [86].

2.3.6 The Flory-Huggins adsorption isotherm

This model (Eq. 21) is believed to be a substitutional model [37,86] because the constant parameter (x) in the equation describes the substitution of inhibitor molecules for water molecules.

$$\theta = \frac{KC}{x-KC} \quad (21)$$

The linearized form has been written in any of the following ways:

$$C/\theta = x/K - C \quad (22)$$

$$\log C/\theta = \log K + x \log (1-\theta) \quad (23)$$

where x is a constant associated with number of molecules of water displaced and consequently the number of molecules of the inhibitor adsorbed. A plot of log C/θ against log (1-θ) should yield linear curves (Fig. 7) which slope gives x and K can be obtained from intercept.

The value of x is used to represent the number of molecules occupying an active site or the number of water molecules initially adsorbed on the metal surface and displaced by the inhibitor molecules [37]. Other forms in which the equation has been written are:

$$C/\theta = Kx(1-\theta) \quad (24)$$

$$\frac{\theta}{1-\theta} = KxC \quad (25)$$

$$\log\left(\frac{\theta}{1-\theta}\right) = \log K + x \log C \quad (26)$$

2.3.7 The Frumkin adsorption isotherm

The Frumkinian approach applied to the adsorption of corrosion inhibitors on metal surfaces has been explained in detail by Bastida et al. [87] and expressed in Eq. 27:

$$KC \propto \frac{1}{1-\theta} e^{\frac{\theta}{1-\theta}} \quad (27)$$

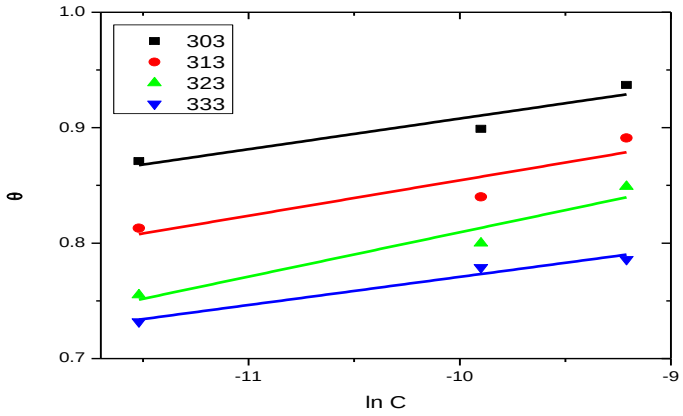

Fig. 5. Temkin adsorption isotherm for inhibition of mild steel corrosion in 2.0 M HCl by different concentrations of 5-HTP at temperatures 303 K to 333 K [27]

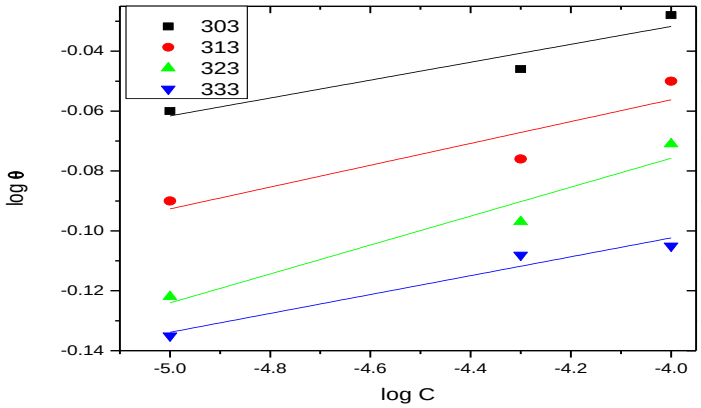

Fig. 6. Freundlich adsorption isotherm for inhibition of mild steel corrosion in 2.0 M HCl by different concentrations of 5-HTP at temperatures 303 K to 333 K [27]

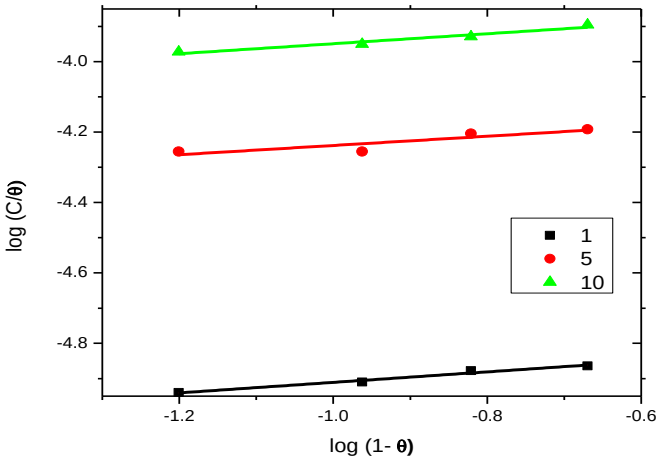

Fig. 7. Flory-Huggins adsorption isotherm for inhibition of mild steel corrosion in 2.0 M HCl by different concentrations of 5-HTP at temperatures 303 K to 333 K [27]

Eddy and Ebenso [88] reported a linearized or 'optimized' form (Eq. 28) which takes the interaction between the adsorbed inhibitor molecules into consideration, given by

$$\log \frac{\theta}{1-\theta}.C = \log K + {}^{2\alpha\theta}/_{2.303} \quad (28)$$

where α is the lateral interaction parameter that describes the interaction in the adsorbed layer. According to widely held views about Eq. 28, the molecular interaction parameter can assume positive or negative values: when $\alpha < 0$, there is repulsion in the adsorbed layer, and otherwise attraction [88-90]. This may be illustrated using 5-HTP (Fig. 8).

2.3.8 The El-Awady adsorption isotherm model

This model is also referred to as the kinetic/ thermodynamic model and is written as follows [91-93]:

$$\log \frac{\theta}{1-\theta} = \log K^* + y \log C \quad (29)$$

where y represents the number of inhibitor molecules occupying one active site of the metal surface. Linear plot (Fig. 9) can be obtained and used to determine the associated parameters like the reciprocal of y which is used to describe the number of active sites on the surface occupied by one molecule of the inhibitor. It can be related to the binding constant, *B*, according to eq. 30.

$$B = K^{\frac{1}{y}} \quad (30)$$

When $\frac{1}{y} > 1$, each inhibitor molecule is believed to occupy more than one active site on the metal surface and vice versa [93].

2.4 Choice of Appropriate Adsorption Isotherm Model

The routine involves fitting the surface coverage data into different adsorption models and the isotherm that best fits the data is used to describe the adsorption behaviour. The best fit is usually the one that gives the highest regression coefficient (R^2) value from the linear plots [94-100]. Depending on the plot tool or software used, other coefficients for assessing fittings such as Adjusted R-square and Pearson's (*r*) values could be used, though related report is scanty in the literature. There are also cases where one or more isotherms are used without necessarily testing the best fit in terms of this criterion [28]. Where such happens, the aim may be to describe parameters of interest associated with the isotherm model employed.

2.5 Determination of Associated Thermodynamic Parameters

The adsorption-desorption constant also called inhibitor-metal binding constant, is usually related to the free energy change of adsorption (ΔG_{ads}) using Eq. 31 or 32.

$$K_{ads} = - \log C_w - \frac{\Delta G_{ads}}{RT} \quad (31)$$

$$\Delta G_{ads} = \left(\frac{1}{55.5}\right) exp^{-\frac{K_{ads}}{RT}} \quad (32)$$

where C_w is the molar concentration of water expressed in g/L, R is the molar gas constant in $Jmol^{-1}K^{-1}$ and T is the absolute temperature (in Kelvin). The value of ΔG_{ads} may be obtained by direct substitution of the variables involved (taking the molar concentration of water to be 55.5 [51,55]) or by a plot of K_{ads} against the reciprocal of T and ΔG_{ads} obtained from slope. It may be more convenient to calculate ΔG_{ads} at a given temperature using the equation below:

$$\Delta G_{ads} = -RT \ln 55.5\, K_{ads} \quad (33)$$

Other parameters like enthalpy and entropy of adsorption denoted by ΔH_{ads} and ΔS_{ads} respectively are obtained from appropriate linear plots using thermodynamic models, some of which are given below [52,60]:

$$\ln K_{ad} = \frac{-\Delta H_{ads}}{RT} + \frac{-\Delta S_{ads}}{R} - \ln C_w \quad (34)$$

$$\ln K_{ad} = \frac{-\Delta H_{ads}}{RT} + \text{constant} \quad (35)$$

$$\Delta G_{ads} = \Delta H_{ads} - T\Delta S_{ads} \quad (36)$$

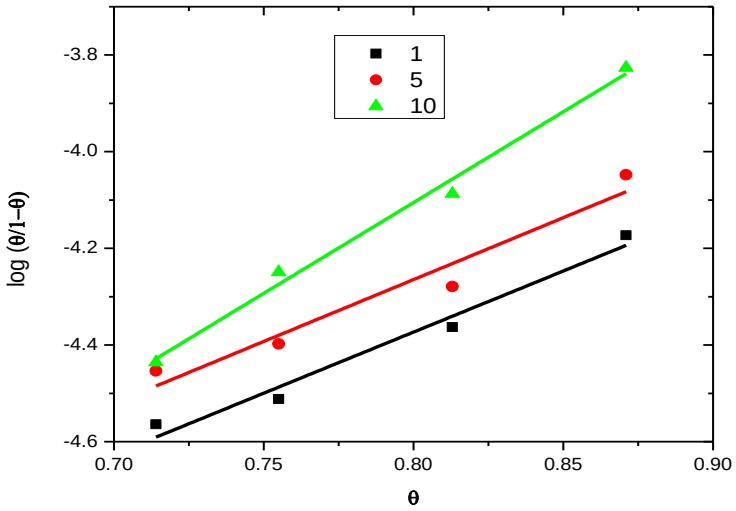

Fig. 8. Frumkin adsorption isotherm for inhibition of mild steel corrosion in 2.0 M HCl by different concentrations of 5-HTP at temperatures 303 K to 333 K [27]

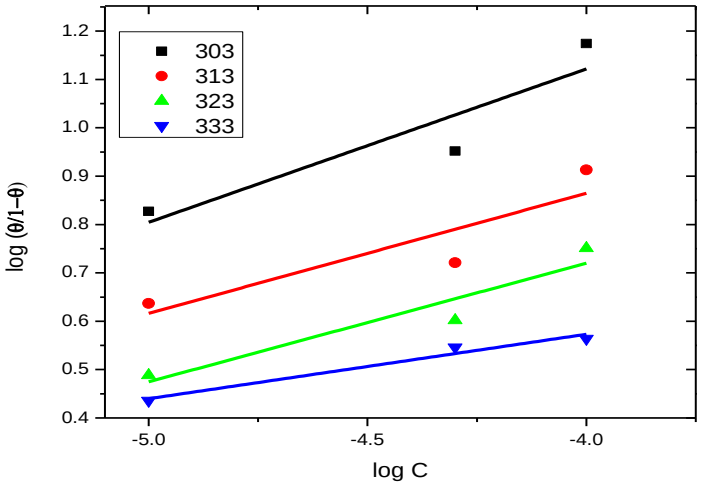

Fig. 9. El-Awady adsorption isotherm for inhibition of mild steel corrosion in 2.0 M HCl by different concentrations of 5-HTP at temperatures 303 K to 333 K [27]

2.6 Prediction of Mechanism of Adsorption and Inhibition

2.6.1 Use of change in free energy of adsorption

Negative values of ΔG_{ads} show that the inhibitor molecules are spontaneously adsorbed on the metal surface, otherwise means non-spontaneous. The mechanism of adsorption is physisorption when the value of $\Delta G_{ads} \leq -20$ kJmol^{-1} and chemisorption when $\Delta G_{ads} \geq -40$ kJmol^{-1} [101-104]. Values in between this range are usually attributed to mixed mechanism or what sometimes called physiochemisorption [105,106]. Mixed mechanism implies that both physical and chemical adsorption occurs simultaneously. Some authors have also predicted the mechanism from absolute values of ΔG_{ads} where the adsorption is believed to follow a physical mechanism when $/\Delta G_{ads}/ \leq 20$ kJmol^{-1}, chemical adsorption when $/\Delta G_{ads}/ \geq -40$ kJmol^{-1} and both mechanisms when $20 \geq /\Delta G_{ads}/ \leq$ -40 kJmol^{-1} [107-109]. Thermodynamically, negative values of heat of adsorption imply exothermic nature with the evolution of heat, otherwise, endothermic. Changes in entropy may be positive or negative corresponding to increase or decrease in disorder of the system.

2.6.2 Other methods of predicting mechanism

The mechanism of inhibition has also been predicted from the trend of activation energy and inhibition efficiency. If the activation energy of the uninhibited solution is denoted by E_u and that of the inhibited solution by E_i, then the mechanism of adsorption is believed to be physisorption if $E_i > E_u$ and inhibition efficiency decreases with temperature increase or chemisorption if $E_i < E_u$ and inhibition efficiency increases with increase in temperature [110].

The use of this approach may not be reliable as trend of inhibition efficiency is believed to provide a single but insufficient justification for the mechanism so proposed. Sometimes, mechanism of inhibition may be predicted from the trend or sign of enthalpy of adsorption. Adsorption enthalpies are dependent on the compounds which would interact with the metal via adsorption, and the nature of the interaction or bond formed. They may quantitatively denote physisorption if less than zero since exothermicity may imply formation of new bonds and evolution of heat and vice versa [111]. It is also believed that the mechanism is physisorption if heat of adsorption is less negative than -40kJmol^{-1} and chemisorption, if enthalpy of adsorption is more negative than -100 kJmol^{-1}.

Recently, a new approach has been proposed based on the degree of responsiveness of inhibitor to change in temperature. This is defined using a parameter called temperature coefficient of inhibition efficiency (μ) [112]. According to this model, negative values of μ signify physical adsorption and positive, chemisorption. Derived by mimicking the classical temperature coefficient of resistance of conductors, the model assumes that a linear relationship exists between the inhibition efficiency (Y) and temperature changes (X), which may be direct $Y = f(X)$ or inverse $Y = f^{-1}(X)$. The fractional change in inhibition efficiency per unit initial efficiency per unit rise in temperature describes μ, and is expressed as

$$\mu = \frac{I_T - I_0}{I_0 \Delta T} \quad (37)$$

where I_0 is initial inhibition efficiency at temperature T_0, I_T is inhibition efficiency at a new temperature T and ΔT is change in temperature, and the linearized form is given in Eq. 38. This model remains open for further tests/criticisms to ascertain its suitability.

$$I_T = I_o \mu \Delta T + I_o \quad (38)$$

3. RESULTS FROM APPLICATION OF ADSORPTION ISOTHERMS TO CORROSION INHIBITION STUDIES

In this section, we have considered some published results from different studies using the isotherms discussed to report adsorption of various corrosion inhibitors. Emphases have not been laid on the performance or effectiveness of the inhibitor but rather on how some of the adsorption parameters were obtained and used to describe inhibitor molecules-metal surface interactions. Corroboration between inhibition efficiency and the trends observed using these parameters (as reported by the authors) have been mentioned. Some concerns have also been raised where the accounts and/or methods of application appear inconsistent with the theory in opinion of the authors. However, in doing this, deliberate efforts have been made as much as possible to avoid undue scrutiny of results.

3.1 Langmuir Adsorption Isotherm

The Langmuir isotherm is perhaps the most frequently used isotherm for corrosion inhibitors because of its simplicity and the widespread understanding of the assumptions underlying its derivation. The isotherm has been used to explain the adsorption of chalcone derivatives on carbon steel in 1.0 M HCl because higher correlation coefficient (R^2) was obtained compared to other models tested [55]. Non-unity slope was obtained and attributed to otherwise interactions between adsorbed species on carbon steel surface and changes in adsorption heat which increased the surface coverage [113,114]. Factors that were ignored in derivation of the model were considered as causes of deviation from unity. The free energy of adsorption values ranged from -36.2 to -36.7 kJmol^{-1}, attributed to charge sharing or transfer from the inhibitor molecules to the metal surface to form covalent bond [115] and a resulting physisorption and chemisorption (or mixed) mechanism.

Mourya et al. [60] also used the Langmuir isotherm for the adsorption of *Tagetes erecta* extracts on mild steel in 0.5 M H_2SO_4. Claiming that it is the most fundamental, their surface coverage data obtained from potentiodynamic polarization studies were first tested with the model, R^2 notwithstanding. The values of K_{ads} obtained decreased with increase in temperature. Interaction of the extract with steel surface involved physisorptions (ΔG_{ads} around -25 kJmol^{-1}), electrostatic in character. The positive sign of entropy change obtained was attributed to increase in solvent entropy and more positive water desorption entropy. The observations were thermodynamically consistent and feasible. Positive entropy change was also attributed to predominance of solvent entropy over solute entropy [40] for an almost perfectly Langmuirian behaviour but associated with both chemical and physical adsorption mechanism.

Thermodynamically, it appears inconsistent at all temperatures for a spontaneous adsorption process to be endothermic with negative sign of entropy. This is a trend observed by Yadav et al. [39] as follows: $\Delta S_{ads} < 0$, $\Delta H_{ads} > 0$ and $\Delta G_{ads} < 0$. It was claimed that the negative entropy change indicates an association rather than a dissociation step in formation of activated complex in rate determining step. This implies that a decrease in disorder took place during transition from reactants to activated complex. Association reactions are known to be endothermic with resultant decrease in entropy. However, many association reactions are not spontaneous and could not have resulted in negative free energy change as reported. Such rebuttal, in our opinion, could have been a consequence of direct computations using transition state equation instead of the K_{ads} values obtained from Langmuir adsorption isotherm.

Shaban et al. [52] reported a spontaneous endothermic adsorption of vanillin cationic surfactants as corrosion inhibitors on mild steel at 25°C to 70°C. Non-unity slopes were reported from Langmuir plot informed by R^2 values and were attributed to the occupation of more than one adsorption site by each inhibitor unit, presence of interactions between the adsorbed species in the metal surface and changes in heat of adsorption with increasing surface coverage [114]. The modified Langmuir equation (Eq. 15) proposed by Villamil et al. was applied [116] which they claim takes molecular interactions and changes in heat of adsorption with surface coverage into consideration to correct the deviation from the Langmuirian behaviour. Other authors have also followed suit using the equation which they sometimes refer to as Villamil adsorption isotherm [116-118].

Slopes proximate to unity (1.008) were obtained for pyridazine derivatives on mild steel surface [41] confirming good adherence to the Langmuirian behaviour. High adsorption ability (K_{ads} = 206,100 M^{-1}) was also reported, with free energy change close to -40 kJmol^{-1} attributed to formation of a coordinate covalent bond by charge sharing or transfer from inhibitor to metal surface by means of inhibitor's N, S, and π functionalities [41,119-121]. There was also possible electrostatic interaction between negatively charged metal surface and the protonated molecules-the mixed type of adsorption [122,123].

Ansari and coworkers credited their large values of ΔG_{ads} to strong interactions between inhibitor molecules and metal surface [45]. It is however uncommon to associate ΔG_{ads} instead of K_{ads} with metal-inhibitor interaction. In a similar report, El-Lateef et al. obtained ΔG_{ads} values between -48.3 and -48.7 kJmol^{-1} and proposed chemical adsorption mechanism because the values obtained were greater than -40 kJmol^{-1} [124]. It is believed that Abd El-Lateef and co-workers were likely referring to the absolute values of the free

energies since the reported values could not be greater than -40 kJmol^{-1} benchmark in magnitude.

Most inhibitors show increase in K_{ads} values as temperature decreases and vice versa [120,122-123]. The justification may be that at higher temperatures, desorption rate increases, the inhibitor effectiveness also decreases leading to decreased surface coverage and increased corrosion rate of the metal. However, Mert and coworkers obtained a contrary result: a rather increasing K_{ads} values with increase in temperature and physical adsorption mechanism was predicted [59]. Although variation of inhibition efficiency with temperature has earlier been held not to by itself provide sufficient basis for prediction of corrosion inhibition mechanism, increase in inhibition efficiency with increase in temperature could have been consistent with this prediction, yet such trends are more commonly associated with chemisorption.

We observe from examination of several reports that in applying the Langmuir adsorption isotherm for corrosion inhibitors, the following are worthy checklists:

- the isotherm should as much as possible produce a non-zero intercept otherwise the adsorption phenomenon becomes non-Langmuirian;
- the concentration of the inhibitor should be expressed in standard molarity units: expressing the concentration term in trivial units may result in fuzzy or imprecise inferences;
- The value of K_{ads} should decrease with temperature increase and vice versa, otherwise, parameters so deduced may be unreliable and vary from one report to another.

3.2 Langmuir-Freundlich (L-F) Adsorption Isotherm

This isotherm is considered a hybrid of the Langmuir isotherm. Since Langmuirian behaviour ignores the possibility of heterogeneity of the active adsorptive sites, the account for such inhomogeneity is attempted in this model. In practice, some of the metal coupons are only degreased before use in most studies or less often polished to near mirror surface. There is no guarantee that the metal surface is left homogeneous by the method of surface preparation used, hence the need for a heterogeneity parameter (denoted by *h*). Tian and co-workers [85] observed that their data best fitted into this isotherm. They used the *h* value to characterize the distribution of adsorption energy at different sites on a non-Langmuirian (inhomogeneous) surface. While K_{ads} still described the adsorption-desorption equilibrium constant related to the thermodynamic free energy as earlier discussed, the *h* value accounts for how narrow or wide the adsorption energy is distributed over the surface sites. The closer the value of *h* is to unity, the narrower the distribution of this energy. In their work, they also suggested that both physical and chemical adsorption mechanism were involved, with chemical adsorption taking predominance.

Not so many authors have applied the L-F adsorption model. Kern and Landlot [125] also applied this isotherm to carboxylic-acid based organic inhibitors adsorbed on iron and gold using electrochemical quartz crystal microbalance developed in their laboratory. Deductions from L-F adsorption isotherm showed stronger interactions between inhibitor and iron than gold.

3.3 Freundlich Adsorption Isotherm

This non-ideal model assumes exponential distribution of adsorption site energies [126]. It has also been described using two slightly different expressions from Eq. 19 and 20. The first and popular expression is as given below [24,102,103,127-131]:

$$\theta = KC^n \tag{39}$$

where n is a constant that depends on the characteristics of the adsorbed molecules [131] and has value between zero and unity. The physical implication(s) of n and is rarely reported apart from giving the range of values, $0 < n < 1$. Logarithmic form of the equation affords linear plots where *K* is determined from the ordinate's intercept and used to deduce free energy change of adsorption.

$$\log\theta = \log K + n\log C \tag{40}$$

A possible explanation of Eq. 39 above is that degree of surface coverage of a corrosion inhibitor on a metal surface is proportional to its concentration raised to a constant power dependent on the characteristic of the species at the interface. When values of n fall within the stated range, the adsorption of the inhibitor is

believed to strictly adhere to this model [132]. The value of n has also been associated with the possibility of adsorption or adsorption degree, which is suitable when the isotherm model is described by the second expression shown in Eq. 19 [132-134].

Seifzadeh et al. [132] claims that adsorption is easy when $0 < n < 1$, moderate if $n = 1$ and difficult when $n > 1$. Reports show that n is often a positive non-integer constant [59, 135] which can also be described as the adsorption intensity [133]. A unit value of n shows that partition between two phases involved is independent on concentration (i.e. $\theta = KC$). Under this assumption, $\frac{1}{n}$ less than unity indicates normal adsorption, otherwise, cooperative adsorption. The reciprocal of n has been described as heterogeneity factor – the smaller the value of $\frac{1}{n}$, the greater the expected heterogeneity and values of *n* around 1 to 10 indicate favourable adsorption process [135].

3.4 Flory-Huggins Adsorption Isotherm

The major description provided by this isotherm in addition to K_{ads} is the non-unity deviation from Langmuirian single-molecular adsorption of corrosion inhibitors to a single active site of the metal denoted by x [136-141]. The introduction of x compensates for molecular interactions or formation of more than one layer of the adsorbed inhibitor molecules. Abd El-Rehim et al. obtained x values up to 4 with PMPA in 2.0 M HCl [142]. They initially defined x as the number of molecules occupying one active site but later attributed this value (1.8 to 4.4 at 293 K to 333 K respectively) to 'one molecule attached to one active site' of steel surface. The rationale that led to this inference is unclear. The values of K_{ads} decreased with temperature increase, which was ascribed to the widely held physical adsorption mechanism and desorption of PMPA at elevated temperature. However, one would expect that more than one PMPA molecules adsorbed per active site of the metal from their initial description of x. Again, the number of molecules adsorbed per active site (x) as reported increased with increase in temperature (Table 1), which appears inconsistent with the physical adsorption mechanism earlier proposed since desorption could have taken place at higher temperature.

Although Eq. 21-26 above have been widely used to describe this isotherm, a different version of this model was employed by Abdel-Gaber et al. [138]. The adsorption of their plant (plant or plant extract? on metal surface best fitted into the Florry-Huggins adsorption isotherm which was stated using eq. 41.

$$\frac{\theta}{x(1-\theta)^x} = KC \quad (41)$$

where *K* is the binding constant and x is the size parameter. They claimed that *Chamonite* extract was bulky and so could displace more than one water molecule from the metal surface, hence the bulkier the inhibitor group that adsorbs to the metal surface active site, the greater the value of x. In another study, Umoren and Ebenso plotted the usual $\frac{C}{\theta}$ against $\log(1-\theta)$ and evaluated x (called size ratio) to represent the number of water molecules displaced by one molecule of the adsorbate [139]. With values of x less than one, they suggested that each molecule of the inhibitor occupies less than one active site on the mild steel surface [136], which is similar to that reported earlier [110].

The value of x can also represent number of water molecules displaced by one molecule of the inhibitor [110,140]. In a related study, 1.01 and 1.13 were obtained respectively for x at 303K and 333K [114]. Since the values were close to unity, one molecule of water was believed to be replaced by one molecule of the inhibitor. In the case of beberine [143], x was about 3.5, and it was inferred that adsorption of one beberine molecule displaces three or more molecules of water/iron atoms. In other words, there may have been more than three active/ effective adsorption centres in one bebeerine molecule. The later description seems consistent to a large extent with the assumptions behind the model. The molecular quantity of the adsorbing molecule was also considered [142].

Table 1. Variation of x with temperature for Flory-Huggins [142]

Temperature (K)	293	303	313	323	333
x	1.8	3.1	3.9	4.3	4.4

Literature survey reveals that the parameter x has been variously implicated as follows:

a. number of metal active sites occupied by one molecule of an inhibitor
b. number of inhibitor molecules occupying one active site of the metal
c. the size of the inhibitor approaching an active site of the metal
d. the number of water molecules displaced by an inhibitor molecule

If an inhibitor molecule approaching the metal surface is large, it is likely to displace more than one water molecule and become attached to more than one surface site, thus making the size parameter in (c) above related to the number of metal active sites (a) above. This would however depend on how many active sites are available in the inhibitor molecule. It is possible for a molecule to have more than one potential adsorption functionality for attachment to the metal. Aromatic amino acids for instance may be thought to have active adsorption sites in the aromatic, amine and acid functionalities. Similar cases may apply to some polymers and complex mixture of phytochemicals of plant extracts. If more than one of these sites gets adsorbed onto the metal surface simultaneously, a monolayer adsorption occurs which may be seen as chemisorption. On the other hand, the possibility that more than one molecule occupies one active site of the metal is rather trivial. For instance, consider a metal surface having one (1) active adsorption site, suppose there are three inhibitor molecules (i.e. x = 3) approaching this site, there will therefore arise a probability that one of the three is first being adsorbed. It becomes more trivial if the inhibitor molecules are equivalent, having similar affinities for the site and also having non-zero interactions within themselves.

3.5 Frumkin Adsorption Isotherm

The Frumkinian adsorption isotherm for describing corrosion inhibitors has been written as [87]:

$$KC \propto \frac{1}{1-\theta} exp \frac{\theta}{1-\theta} \quad (42)$$

where all terms retain usual meanings. It can also be written as shown below (Eq. 43), where α is the lateral interaction parameter that describes the interaction in the adsorbed layer and K is the adsorption-desorption equilibrium constant

$$\log \frac{\theta}{1-\theta} . C = \log K + \frac{2\alpha\theta}{2.303} \quad (43)$$

Eddy and Ebenso obtained values of α between 4.16 and 0.07 at 303 K and 333 K respectively and attributed to attractive behaviour of the inhibitor, the strength of which decreases as temperature increases [139]. Martinez and Stern also employed Eq. 43 and reported similar deductions [89]. Valek and Martinez reported that the constant parameters in Eq. 43 could not be calculated because the average molecular mass of the extract used was unknown [90]. Ideally, concentrations should be reported in terms of molarity (M). In practice, for many studies especially involving the use of plant extracts and polymers, expressing concentration in g/dm^3 or other units is considered no problem.

The value of α may also be negative as obtained for AAMTDA ($\alpha = -1.620$) and BTAH inhibitors ($\alpha = -0.898$) and attributed to repulsive forces between the inhibitor and the metal surface [90]. This inference presents another way the constant α can be described. Recently, the relationship below (Eq. 44) has been used for Frumkin isotherm [146]:

$$\frac{\theta}{n(1-\theta)^n} e^{-2\alpha\theta} = KC \quad (44)$$

The term n was introduced to denote the number of water molecules displaced from the adsorbent surface via the adsorption process and α is the Frumkin adsorption parameter. Obviously, the workability of the above equation would depend on what value n assumes. The value of n has been assumed to be 2 or 3 (i.e. non-unity) and other parameters were deduced [146]. A similar approach was also used by Abd El-Rehim et al. [147] and α was obtained from a plot of θ against log C.

De Souza and Spinelli [148] considered that the double-layer capacitance is proportional to the surface not covered by the inhibitor, and so evaluated θ from:

$$\theta = \frac{1-C_i}{C_o} \text{ x } 100 \quad (45)$$

where C_o and C_i are the double-layer capacitance determined without and with the inhibitor. He plotted $\log \frac{\theta}{1-\theta} C$ against θ from Eq. 46 below:

$$\log \frac{\theta}{1-\theta} C = \log K - g\theta \quad (46)$$

where g is the adsorbate interaction parameter; K = 1058.5 Lmol^{-1} and ΔG = -27.2 kJmol^{-1} were obtained, attributed to spontaneous chemical adsorption because the magnitude of free energy value were in the order of 30 kJmol^{-1}. The data also fitted into Langmuir and Temkin adsorption isotherm.

Vracar and Drazic [149] plotted θ against [log $\frac{\theta}{n(1-\theta)^n}$ – logC], with assumption that $n = 2$ and $n = 3$. Both values yielded straight lines where positive α values were obtained. They reported that α increases with the number of functional groups substituted on the benzene ring of the inhibitor which indicates highly attractive lateral interactions in the adsorbed layer. It was observed that the strength of the lateral interaction increased counter to trend of corrosion inhibition efficiency. Thus, if a vertical orientation on the Fe surface is created, predominant conditions would be physisorption of the sulfonic groups directed towards the surface of the iron, so that chemisorption would be created by horizontal orientation (if present) due to pie electrons-metal interactions.

The values of α has also been used to describe the heterogeneity of the surface and measure of the steepness of the adsorption isotherm [150]. Data generated from weight loss, impedance and polarization studies fitted into the isotherm and were claimed to be in good agreement. The values of K obtained decreased with increase in temperature, a trend that was attributed to physical adsorption, showing that the strength of binding of inhibitor to metal surface decreases as temperature increases. Positive α values were obtained and explained in terms of increased adsorption energy with increased surface coverage as a result of molecular interactions.

Frumkinian binding behaviour of corrosion inhibitors to metal surface has also been explained using Eq. 47 [151,152], where the concentration term was rather placed as a denominator of a natural logarithmic function. Positive α values were also obtained and ascribed to increase in adsorption energy with increase in surface coverage caused by interactions between the molecules. A physical adsorption mechanism was proposed based on decrease in K values with increase in temperature.

$$\ln \frac{\theta}{C(1-\theta)} = \log K - 2\alpha\theta \quad (47)$$

3.6 Temkin Adsorption Isotherm

Temkin adsorption model has also been extensively used for adsorption of corrosion inhibitors because it is believed to account for some of the factors not considered in the Langmuirian model. Basically, the factors 'a' and 'f' have been introduced to account for molecular interactions in the adsorbed layer and heterogeneity of active sites. The general form of the model is represented below:

$$e^{-2a\theta} = KC \quad (48)$$

where a is the molecular interaction parameter and K is the equilibrium constant of the adsorption process. The values of a may be positive or negative and indicate whether attraction or repulsion takes place in the adsorbed layer. Different authors have assigned attractive or repulsive force to the sign of a in different ways. Umoren and Ebenso [139] fitted their experimental data into the Temkin model above and obtained negative values of a in all cases and attributed it to repulsions that take place in the adsorbed layer. The adsorbate-adsorbent strength gave large values corroborating with the better inhibition efficiency obtained and physisorption mechanism [152,153].

Sahin et al. applied adsorption isotherms to describe their cyclic nitrogenous inhibitor compounds on mild steel [154]. The surface coverage data of two of the inhibitors (coded TTA and 2-ABA) best fitted into the Temkinian model in NaCl solution. The inhibition efficiencies of the compounds were rationalized under the assumption that:

- the inhibition is a result of coverage of the metal surface by inhibitors, making contact with the corroding medium difficult; and
- the coordination of pie electron system in the inhibitor moiety facilitates the attachment of molecules on metal surface.

No information was provided on the data acquired and their significance to the nature of interaction of inhibitors. Durnie et al. [155] employed Temkinian plot over 30-70°C for sixteen (16) organic corrosion inhibitors and obtained equilibrium constant of adsorption, molecular interaction parameter and adsorption enthalpy. It was inferred that molecular interaction constants are dependent on the

charge at the hydrophobic head group of inhibitors as well as steric factors such as length, flexibility and branching of the hydrophobic chain. High molecular interaction constant was obtained, and said to signify strong force of repulsion between adsorbed and adsorbing molecules and its magnitude was related to electrostatic (Columbic) repulsive force experienced by a molecule approaching the surface of a metal to be adsorbed as a result of neighbouring adsorbed molecules. The values of f were used to develop and predict the structure-activity relationship for the sixteen corrosion inhibitors studied. The compounds were all chemisorbed on to the electrode and yielded good film persistency or corrosion protection.

Hosseini et al. obtained better fit for their asymmetrical Schiff base inhibitors using Temkin [R^2 = 0.99] than Langmuir plot, which they claimed could not meet the criteria it was derived for [156]. They opined that Temkin explicitly takes adsorbing species-adsorbate interactions into account. Molecular interaction constant up to 4.71 was obtained with *K* values in the order of 10^6 to 10^4 dm^3mol^{-1} and negative ΔG up to 26 to 27 $kJmol^{-1}$ but the molecular interaction parameter was calculated as f instead of a. In another report, a was claimed to be dependent on the molecular interaction among the adsorbed particles and surface and the degree of homogeneity of the metal samples [157]. The constant, f, may also be seen as a factor of energetic inhomogeneity (which we have represented using $f = f^I\{-a\}$ according to Obot and Obi-Egbedi [25]. However, there was no quantitative description of the range of values or sign of a that corresponds to a given measure of inhomogeneity of the metal surface.

The Temkinian model has also been expressed as:

$$\ln KC = \alpha\theta \tag{49}$$

where α is the molecular interaction parameter which may be positive or negative in sign depending on the the steepness of the the resulting adsorption isotherm [158]. The more positive α value is, the steeper the isotherm slope. Interactions between molecules with positive α values cause an increase in adsorption energy with increase in surface coverage. It was claimed that *K* values deduced from the isotherm were incompatible. The word 'incompatible' as used is unclear, except if it implies that Temkin model is only applicable to cases where one active site per molecule is occupied. The obtained α values were positive while ΔG values gave a high efficient spontaneous adsorption.

3.7 El-Awady Adsorption Isotherm Model

Often referred to as kinetic/thermodynamic adsorption isotherm model, this model introduces a new constant parameter expressed in terms of y used to denote the number of inhibitor molecules occupying one active site [138]. It describes a non-monolayer adsorption, where more than one molecule can occupy an active site of the metal depending on the value of y. The model is expressed as follows:

$$\frac{\theta}{1-\theta} = K^* C^y \tag{50}$$

$$\log\frac{\theta}{1-\theta} = \log K^* + y\log C \tag{51}$$

and

$$K^{*(1/y)} = K_{ads} \tag{52}$$

Abdel-Gaber et al. [138] reported that some of the plants extract studied as inhibitors fitted into other adsorption models. For instance, kidney bean nut extract fitted into Langmuir, Chamomile extract fitted into Flory-Huggins but all the extracts also fitted into the kinetic-thermodynamic model. The number of active sites occupied by a single molecule is denoted by $\frac{1}{y}$ so that y denotes the number of molecules on an active site of a metal. Values of $\frac{1}{y}$ obtained were nearly equal to the size parameter (x) in the Flory-Huggins model for the adsorption of Chamomile extract and the binding constants obtained were in close agreement with that of Langmuir and Flory-Huggins.

When $\frac{1}{y} < 1$, multilayer adsorption takes place and when $\frac{1}{y} > 1$, one inhibitor molecule occupies more than one active site. The later suggests the possibility of the adsorbing molecule possessing more than one active adsorption centres. Foad et al. [159] obtained $y \approx 1$ at all the temperatures studied and assumed the occupation of one active site by a single molecule with strength of adsorption (from *K* values) decreasing with increasing temperature. The values of $\frac{1}{y}$ obtained were also close to unity and imply the formation

of multilayers of the inhibitor on the metal surface. In other words, values of y far less than one would mean that a given inhibitor molecule would occupy more than one active site, portraying $\frac{1}{y}$ as the number of active sites occupied by one inhibitor molecule.

The value of $\frac{1}{y}$ might increase with increasing degree of surface coverage [160-161]. Values of $\frac{1}{y}$ reported for exudate of Umoren et al. [162] were more than unity and was implied that each molecule of the phytochemical compounds from the exudate involved in the adsorption process is attached to one active site on the metal. Similar result ($\frac{1}{y} > 1$) was also reported for naturally occurring exudate gums [92] though each molecule of the phytochemical was attached to more than one active site. Such contradictions in the explanation of the significance of $\frac{1}{y}$ values are common in literature. For instance, values of $\frac{1}{y}$ obtained with spontaneous adsorption of phenylthiazole on steel surface ranged from 3.1 to 6.9 and was explained that a given inhibitor molecule will occupy more than one active site [93]. Value of $\frac{1}{y}$ as large as 8.29 was also obtained [163] and explained that sulphate ions are more hydrated compared to chloride ions, therefore, are poorly adsorbed on the positively charged metal (iron) surface, leaving more active sites for the adsorption of the inhibitor, resulting in the large number of adsorbing sites available for the inhibitor (approximately 9 sites).

This model is more often used complementary to other models like Temkin, Langmuir or Frumkin isotherm [164-169] because there are rare cases where the adsorption of a given corrosion inhibitor is explained using this isotherm alone. We have also observed from many reports reviewed that when obtained $\frac{1}{y}$ values are less than unity [170] or some are less while others are greater than unity for the same inhibitor [171], such reports ignore are usually ignored. We therefore recommend investigation into possible explanations to such trends in future researches.

Unlike with other models discussed so far, most reports using El-Awady model follow a consistent version according to Eq. 49-51 above. However, a different version (Eq. 53) was reported and claimed to be obtained from the kinetic point of view by Moussa et al. [157].

$$\frac{\theta}{1-\theta} = \left[\left(\frac{K_o}{K_{abs}}\right) - 1\right] \quad (53)$$

But,

$$\log\left(\frac{K_o}{K_{abs}} - 1\right) = \log K + y \log C \quad (54)$$

where K_o is rate constant at zero inhibitor concentration, K_{obs} is observed rate constants for the reactions with inhibitors, y is the number of inhibitor molecules occupying one active site and K was obtained from the rate equation (Eq. 55). Sadly, the results so obtained were not communicated.

$$\text{Rate of reaction} = KC^n \quad (55)$$

3.8 Adsorption Isotherms of the 5-HTP Experiment

In the preceding sections, we have described how many parameters associated with various adsorption isotherms have been used to explain the nature of interaction between metal adsorbents and corrosion inhibitor. In this section, we have extracted data from an earlier report [25] on the inhibition of mild steel corrosion by 5-HTP analysed and fitted same into some isotherm models discussed. The results obtained have been used to illustrate implications of the parameters obtained (Tables 2-3).

From Langmuir adsorption isotherm, non-unity slopes were obtained. Both plots (a) and (b) yielded slopes of 5.1 to 4.7 and 0.10 to 0.17 respectively with values decreasing as temperature increased. This may be attributed to either inhomogeneity of the metal surface or difference in adsorption enthalpies (affinities) of the sites. Non monolayer adsorption is therefore expected with possible interactions between either the sites or the adsorbed molecules. These are factors that were not considered during the derivation of the model.

The decrease in slope values with increase in temperature may be associated with decrease in number of inhibitor molecules adsorbed on the steel surface as temperature increases. Decrease in strength of adsorption with increase in temperature is inferred from the trend of adsorption equilibrium constant. It may also be deduced from the modified Langmuirian parameters that more than one molecule may have occupied a given active site of the metal and the amount decreases with temperature, perhaps due to increased desorption rate.

With Freundlich model, the values of *n* were above the zero-to-unity range as earlier stated. However, at low temperatures, *n* tends to unity which may suggest that adsorption is easy at low temperature and perhaps difficult at high temperature. Negative values of Temkinian molecular interaction parameters showed that repulsion takes place in the adsorbed layer with decrease in adsorption energy as temperature increased. Values of *y* obtained using El-Awady model suggests that more than one molecule occupies an active site of the metal. The size parameter obtained from Flory-Huggins model may imply that the size of the adsorbed inhibitor molecule is small, though the values show no specific trend. Frumkin isotherm yielded negative values of *α* which implies that there are lateral repulsive interactions between adsorbed inhibitor molecules which increases with inhibitor concentration, and this is consistent with results obtained using Temkin isotherm. Generally, values of K_{ads} obtained for all isotherms decreased with increase in temperature, pointing to possible decrease in the rate of condensation of the 5-HTP molecules on the steel surface possibly due to high temperature which induced desorption.

The various adsorption isotherms of best fit for other inhibitors reported in some of the papers reviewed have been listed in Table 4. Except different adsorption inhibitors from different origin behave differently, there is need for a consensus approach or definition of the parameters associated with adsorption isotherms models. This would help in making recommendations or drawing inferences universally. Also, where necessary, the concentration of the inhibitor should be expressed in molarity term. These would remove ambiguity in results and generalize inferences drawn from the calculated parameters.

Table 2. Parameters deduced from other adsorption isotherms using results reported for 5-HTP [27]

Model	Parameters	303K	313 K	323 K	333 K
	Slope	5.01	4.95	4.90	4.76
Langmuir (a)	K_{ads}	0.341	0.306	0.277	0.268
	R^2	0.9981	0.9981	0.9950	0.9811
	Slope	0.17	0.14	0.13	0.10
Langmuir (b)	K_{ads}	0.4460	0.441	0.330	0.231
	R^2	0.9746	0.9514	0.9941	0.8531
	n	5.01	4.95	4.90	4.76
Modified Langmuir	K_{ads}	1.709	1.514	1.356	1.276
	R^2	0.9789	0.9717	0.9216	0.9556
	n	6.25	5.00	3.92	1.56
Freundlich	K_{ads}	0.967	0.966	0.975	0.838
	R^2	0.9981	0.9987	0.9956	0.9811
	a	-0.751	-0.642	-0.210	-0.186
Temkin	K_{ads}	6.860	5.888	5.097	5.149
	R^2	0.8907	0.9512	0.8794	0.9386
	y	5.0	4.9	4.9	4.8
El-Awady	K_{ads}	0.4460	0.441	0.330	0.231
	R^2	0.9746	0.9514	0.9941	0.8531

Table 3. Flory-Huggins and Frumkin adsorption parameters obtained for 5-HTP [27]

5-HTP concentration	Flory-Huggings			Frumkin		
	x	K_{ads} x 10^{-5}	R^2	*α*	K_{ads} x 10^{-7}	R^2
1.0 x 10^{-5} M	0.149	1.732	0.9903	-2.9	4.074	0.9875
5.0 x 10^{-5} M	0.131	7.834	0.8910	-2.9	4.898	0.9750
10.0 x 10^{-5} M	0.141	15.596	0.9763	-4.3	7.762	0.9955

Table 4. Various adsorption isotherms for different corrosion inhibitors on different adsorbents in several aggressive media

Metal adsorbent	Corrosion inhibitor (Adsorbate)	Corroding media	Adsorption isotherm	Ref.
MS	Marigold flower extract	0.5M H_2SO_4	Langmuir	[60]
MS	2-amino-4-methylpyridine	0.5M H_2SO_4	Langmuir	[141]
MS	Vanillin cationic surfactants	1 M HCl	Langmuir, Villamil	[52]
Euronorm: C3SE CS and specification: SAE 1035	Pyrimidothiazine derivative	2M H_3PO_4	Langmuir	[172]
CS strips	Chalcone derivatives	1M HCl	Langmuir	[57]
MS	Poly vinyl-alchohol-grafted poly (acrylamide-vinyl sulfonate)	1 M HCl	Temkin	[58]
MS	2-amino ehanethiol	0.1 M HCl	Langmuir	[51]
Aluminium (99.99%)	Imidazole derivatives	0.5 M HCl	Frumkin	[61]
MS	Chemically modified lignin polymers from *Elaeis guineenses*	0.5 M HCl	Langmuir	[173]
MS	Tetrazolo[1,5-α]quinolone-4-carbaldehyde and its Schiff base	1 M HCl	Langmuir	[174]
Aluminium	Extract of Rosemary leaves	Biodiesel	Langmuir	[175]
Steel	Extracts of Chamomile, Halfabar, Black cumin and Kidney bean	1 M H_2SO_4	Langmuir, Flory-Huggins, El-Awady	[138]
N-80 and MS	Fatty acid triazoles	15% HCl	Temkin	[176]
N-80 and MS	5-salicyliadeneamino-3-hydrazino-5-mercapto-1,2,4-triazole (SAHMT)	15% Boiling HCl	Temkin	[177]
MS	*Hibiscus rosa sinensis* leaves extract	2 M HCl	Freundlich, Langmuir, Temkin	[178]
MS	Acenaphtho[1,2-b]quinoxaline and acenaphtho[1,2-b]pyrazine	1 M H_2SO_4	Langmuir	[28]
MS	Poly propylene glycol/silver nanoparticle composite	0.5 H_2SO_4	Temkin	[30]
MS	Xnathan gum and surfactant additives	1 M HCl	Langmuir	[31]
MS	o-fumaryl-chitosan	1 M HCl	Langmuir	[33]
MS	Benzalkonium chloride	0.1 M H_2SO_4	Langmuir	[36]
Euronorm: C3SE CS and specification: SAE 1035	Alkaloids extracts of *Retama monosperma (L) Boiss*	1 M HCl	Langmuir	[179]
C1018 steel	Phenolic Schiff bases	3.5% NaCl + 0.1 M HCl	Langmuir	[180]
Cylindrical MS	Schiff base molecules	1 M HCl	Langmuir	[181]
MS	Pyridazine derivatives	1 M HCl	Langmuir	[41]
MS	Schiff bases of isatin	20% H_2SO_4	Langmuir	[182]
N-80 steel	Pyridine derivatives	15% HCl	Langmuir	[38]
MS	Pyridine derivatives	15% HCl	Langmuir	[39]
MS	5-(phenythio)-3H-pyrole-4-carbonitriles	1 M HCl	Langmuir	[183]
MS	Triazole Schiff bases	0.5 M HCl	Langmuir	[40]
Pipeline steel	Commercially available inhibitor	CO_2 in turbulent flow	Langmuir	[184]
MS	(+)R and (-)S enantiomers of racemic amisulphride	1 M HCl	Langmuir	[185]

Metal adsorbent	Corrosion inhibitor (Adsorbate)	Corroding media	Adsorption isotherm	Ref.
C1018	Naphthenate surfactants based on petroleum acids and nitrogenous bases	CO_2 saturated brine	Langmuir	[124]
MS	[N-substituted]p-aminoazobenzene derivatives	1 M H_2SO_4	Langmuir	[187]
Steel-copper sample	*Curcuma longa* extract	Petroleum waste water	Temkin	[188]
CS37	Surfactants incorporated with 1,3,5-triethanolhexahydro-1,3,5-triazine	1 M HCl	Langmuir	[189]
Alloy steel	Imidazoline based indicator	3wt.% NaCl + CO_2	Langmuir	[190]
MS	Diphenolic schiff bases	0.1 M HCl	Temkin	[186]
MS	Bis(indolyl)methanes	1 M HCl	Langmuir	[105]
MS	Watermelon waste product extract	1 M HCl	Langmuir	[191]
304 stainless steel	*Santolina chamaecyparissus* extract	3.5% NaCl	Langmuir	[192]
J55 steel	A tetrone macrocyclic compound	3.5% NaCl	Langmuir	[193]
MS	Aryl sulfonamidomethylphosphonates	1 M HCl	Langmuir	[1]
CS	Non-ionic surfactants based on tolytriazine	Formation water	Langmuir	[84]
Copper	Triazolyl-acyl hydrazine derivatives	Chloride solutions	Langmuir, Freundlich	[85]
CS	Sulfidated poly (acrylamide-vinyl acetate	1 M HCl	Langmuir	[194]
MS	Halogen substituted imidazole derivative	0.5 M HCl	Langmuir	[195]
MS	Azomethine compounds	1 M HCl	Langmuir	[196]
MS	*Nicotiana talcum* leaves extracts	2 M H_2SO_4	Langmuir	[197]
API 5LX52	Imidazolic ionic liquids	1 M HCl, 1 M H_2SO_4	Langmuir	[198]
MS	Organo-cyclic aldehydes and blends	CO_2– 0.5MNaCl (40-120°C), 1atm–10ar; 1,4,7.7MHCl, 0.5MH_2SO_4	Langmuir	[199]
MS	Thiazolo-pyrimidine derivatives	1 H H_2SO_4	Langmuir	[200]
N-80	Triazine derivatives	15% HCl	Langmuir	[201]
CS	1-dodecyl-4-(((3-morpholinopropyl)imino)methyl)pyridine-1-ium bromide	7 M H_3PO_4	Langmuir	[202]
MS	Seeds and leaves extracts of *Griffonia simplicifolia*	1 M and 15% HCl	Temkin Freundlich	[203]
CS	*Artemisia mesatlantica* essential oil	1 M HCl	Langmuir	[167]
Zinc	Nonionic surfactants	7 M KOH	Freundlich	[86]
Q235 CS	*Capsella bursa-pastoris* extract	1 M HCl	Langmuir	[204]
MS	Xanthan gum and its grafted copolymer	15% HCl	Langmuir	[205]
CS	Antibacterial drugs	1 M HCl	Langmuir	[206]
Aluminium	Some purines	0.1 M HCl	Flory-Huggins, El-Awady	[207]
MS	Indigo dye + halide ions	0.2 M H_2SO_4	Frumkin, Flory-Huggins	[37]
Copper	4-amino-antipyrine	3 wt.% NaCl	Langmuir	[208]
Concrete steel reinforcement	EDTA disodium salt	3.5% NaCl	Langmuir , Freundlich, El-Awady	[209]
Aluminium	2-acetylphenothiazine + Halide ions	0.1 – 0.5 M H_2SO_4	Flory-Huggins	[109]

Metal adsorbent	Corrosion inhibitor (Adsorbate)	Corroding media	Adsorption isotherm	Ref.
MS	4-(2^{l}-amino-5^{l}-methylphenylazo)antipyrine	2 M HCl	Flory-Huggins	[142]
MS	Polyacrylamide +Iodide ions	1 M H_2SO_4	Freundlich, Temkin, Flory-Huggins	[139]
Low CS	*Mimosa tannin* extract	0.1 M H_2SO_4	Flory-Huggins	[137]
Steel	Schiff base with its cobalt complex	1 M H_2SO_4	Langmuir, FloryHuggins, El-Awady	[210]
Zinc	Ethoxylated fatty acids	1 M HCl, 1 M H_2SO_4	Langmuir, Flory-Huggins, Freundlich, Frumkin, El-Awady	[159]
MS	*Citrus aurantifolia leaves extract*	1 M HCl	Flory-Huggins	[140]
C1018 steel	Decylamides of α-amino acids	1 M HCl	Flory-Huggins	[211]
Aluminium	Methylene blue + KCl, KBr, KI	2 M HCl	Langmuir, Flory-Huggins	[114]
Steel	Cyclic nitrogenous compounds	2.5% and 3.5 % NaCl	Langmuir	[154]
MS	Berberine	1 M H_2SO_4	Flory-Huggins	[144]
MS	Congo red dye + KCl, KBr, KI	2 M H_2SO_4	Flory-Huggins	[143]
Low CS	Octylphenol polyethyleneoxide	0.5 M H_2SO_4	Flory-Huggins	[212]
Low CS	Mimosa tannin	H_2SO_4 (pH = 1 and 3)	Temkin, Freundlich, Frumkin	[89]
MS	Methionine	0.5 M H_2SO_4	Temkin, Langmuir	[213]
MS	Extract of *Musa sapientum*	2.5 M H_2SO_4	Langmuir, Frumkin	[145]
Steel	Pennyroyal oil from menthe pulegium	1 M HCl	Frumkin	[214]
CS	Cationic surfactants and inorganic anions	Formation water (pH=6.7)	Flory-Huggins, El-Awady	[141]
CS	Pyrazolone derivatives + KI, KSCN, KI	2 M HCl	Frumkin	[146]
Copper	*Azadiracthta indica* leaves extract	0.5 M H_2S0_4	Frumkin	[90]
Aluminium	Ethoxylated fatty acids	1M HCl	Frumkin	[216]
Iron electrode	Naphthalene and naphthol disulfuric acid derivatives	0.5 M H_2S0_4	Frumkin	[149]
Aluminium	1,1(laurylamido)propylammonium chloride	1 M HCl	Frumkin	[147]
Copper	Triphenylmethane derivatives	1 M H_2S0_4	Frumkin, El-Awady	[152]
MS	Nitrogenous organic molecules	Carbonated brine	Temkin	[155]
Aluminium	Sodium dodecylbenzene sulphonate	1 M HCl	Frumkin	[150]
MS	Assymetrical Schiff bases	0.5 M H_2S0_4	Temkin	[156]
Pure aluminium	dodecylphenolethoxidate	1 M HCl	Frumkin, El-Awady	[215]
MS	Ketoconazole	0.1 M H_2SO_4	Langmuir	[162]
Aluminium	Exudate gum from *Raphia hookeri*	2 M HCl	Temkin, El-Awady	[217]
MS	Ceftazidime	1 M HCl	Langmuir, El-Awady	[171]
MS	Disulfram	1 M HCl	Langmuir, El-Awady	[170]
304 stainless steel	4-phenylthiazole derivatives	3 M HCl	Temkin, El-Awady	[93]

Metal adsorbent	Corrosion inhibitor (Adsorbate)	Corroding media	Adsorption isotherm	Ref.
Pure aluminium	Naturally occurring exudate gums	2 M HCl	Temkin, El-Awady	[92]
CS	Thiosemicarbazide and its derivatives	2 M HCl	Temkin, El-Awady	[160]
CS	Some organic surfactants	Formation water	Flory-Huggins, El-Awady	[217]
Al-6063	Some pharmaceutical compounds	0.5 M H_3PO_4	Frumkin, Temkin	[218]
Pure iron	Polyacrylamide	0.5 M H_2SO_4	El-Awady	[163]
CS	Water soluble hydrazines	0.1 M HCl	Temkin, El-Awady	[157]
MS	sulphamethoxazole	1 M HCl	El-Awady, Flory-Huggins	[161]
Aluminium	Some anionic surfactants	1 M HCl	Freundlich	[102]
Aluminium AA1060	Gingseng root	1 M HCl	Freundlich	[127]
Aluminium	*Sansevieria trifasciata* extract	2 M HCl	Freundlich	[103]
MS	Nizoral derivatives	0.1 M H_2SO_4	Langmuir, El-Awady	[219]
MS	Polyvinyl pyrrolidone +halide additives	1 M H_2SO_4	Freundlich, Temkin	[24]
MS	*Sida acuta* extract + iodide ions	1 M H_2SO_4	Freundlich	[130]
Vanadium	Some amino acids	Solutions with pH of 2, 7 and 12	Freundlich	[131]
Magnessium	Schiff base	0.1 M HCl	Freundlich	[132]
Copper-nickel alloy	Benzotriazole	5% HCl	Langmiur, Freundlich, El-Awady	[135]
CS	Thiosemicarbazole derivatives	2 M HCl	Freundlich, El-Awady	[101]
Tin	Some amino acids	Tartaric acid (pH=1.8)	Freundlich	[104]
MS	Fenugreek leaves extract	2 M H_2SO_4, 2M HCl	Temkin (H_2SO_4), Langmuir (HCl)	[106]
MS	Nevirapine	1 M HCl	Langmuir	[113]
MS	*Piper guineensis* extract	1 M HCl, 1 M H_2SO_4	Langmuir	[117]
Aluminium	*Aningeria robusta* extract + iodide ions	2 M HCl	Langmuir	[118]
MS	Polrhodanine-N-acetic	0.1 M HCl	Langmuir	[119]
MS	Benzotriazole, aminotriazole and 1,2,4-triazole	0.1 M each of HCl, H_2SO_4, H_3PO_4, HNO_3	Langmuir	[126]
Copper	Benzotriazole	0.001 M, 0.005 M and 0.01 M H_2SO_4	Frumkin	[87]
Aluminium	Fluconazole	0.1 M HCl	Temkin	[25]

4. CONCLUSION

Adsorption isotherm models employed to characterize the nature of interactions in the adsorbed layer between corrosion inhibitors and metal surfaces were reviewed from published reports for the first time. The models include Langmuir, Modified Langmuir, Freundlich, Langmuir-Freundlich, Temkin, Flory-Huggins, Frumkin and El-Awady. The isotherms

parameters provide information for predicting important interfacial properties such as the number of water molecules displaced by inhibitor molecules, the number of inhibitor molecules occupying an active site, size parameter of inhibitors, attraction or repulsion taking place in the adsorbed layer, monolayer or multilayer adsorption of the inhibitor molecules to the surface and heterogeneity of the surface. The spontaneity of the adsorption process as well as the strength of binding between the protective film form by the inhibitor and the metal surface can also be predicted. Clarifications provided on the proper interpretation of these parameters would eliminate ambiguities and provide clear routes for readers and future researchers.

COMPETING INTERESTS

Authors have declared that no competing interests exist.

REFERENCES

1. Verma C, Pallikonda G, Chakravarty M, Quraishi MA, Bahadur J, Ebenso EE. Aryl sulfonamidomethyl phosphonates as new class of green corrosion inhibitors for mild steel in 1 M HCl: Electrochemical, surface and quantum chemical investigation. J. Mol. Liq. 2015;209:51-59.
2. A Dabrowski. Adsorption - from theory to practice. Adv. Colloid Interface Sci. 2001; 93:135-224.
3. Marti N, Bouzas A, Seco A, Ferri J. Struvite precipitation assessment in anaerobic digestion process. Chem. Eng. J. 2008;141:67-74.
4. De Voorde BV, Bueken B, Denayer J, DD Vos. Adsorptive separation on metal-organic frameworks in the liquid phase. Chem. Soc. Rev. 2014;43;5766-5788.
5. Liu H, Nishide D, Tanaka T, Kataura H. Large scale single chirality separation of single-wall carbon nanotubes by simple gel chromatography. Nat. Comm; 2011. DOI: 10.1038/ncomms1313
6. Roosen J, Binnemans K. Adsorption and chromatographic separation of rare earth with EDTA- and DTPA-functionalized chitosan biopolymers. J. Mater. Chem. 2014;2:1534-1546.
7. Delmas H, Creanga C, Julcour-Lebique C, Wilhelm AM. AD-OX: A sequential oxidative process for water treatment – adsorption and batch CWAO regeneration of activated carbon. Chem. Eng. J. 2009; 152:189-194.
8. Liang Z, Wang YX, Zhou Y, Liu H. Coagulation removal of melanoidins from biologically treated molasses wastewater using ferric chloride. Chem. Eng. J. 2009; 151:88-94.
9. Burger R, Conch F, Tiller FM. Application of the phenomenological theory to several published works experimental cases of sedimentation process. Chem. Eng. J. 2000; 80:105-107.
10. Deuschle TAL, Janoske U, Presche M. CFO-model describing filtration regeneration and deposite rearrangement effects in gas filler systems. Chem. Eng. J. 2008;148:49-55.
11. Valdes H, Romero R, Sanchez J, Bocquet S, Rois GM, Valenzuela F. Characterization of chemical kinetics in membrane-based liquid-liquid extraction of molybdenum (vi) from aqueous solutions. Chem. Eng. J. 2009;151:333-341.
12. Foo KY, Hameed BH. A short review of activated carbon assisted electrosorption process: An overview, current stage and future prospects. J. Harzard. Mater. 2009; 171:54-60.
13. Macfarlane AL, Prestidge R, Farid MM, Chen JJJ. Dissolved air floatation: A novel approach to recovery of organosolvlignin. Chem. Eng. J. 2009;148:15-19.
14. Abdullah MA, Chiang L, Nadeem M. Comparative evaluation of adsorption kinetics and isotherms of a natural product removed by amberhite polymeric adsorbents. Chem. Eng. J. 2009;146:370-376.
15. Miladinovic N, Weatherly LR. Intensification of ammonia removal in a combined ion-exchange and nitrification column. Chem. Eng. J. 2008;135:18-24.
16. Foo KY, Hameed BH. Insights into modeling of adsorption systems. Chem. Eng. J. 2010;156:2-10.
17. Bajpai AK, Rajprot M. Adsorption techniques-a review. J. Sci. Ind. Res. 1999;58:844-860.
18. Misak NZ. Some aspects of the application of adsorption isotherm to ion exchange reactions. React. Funct. Polym. 2000;43: 153-164.
19. Misak NZ. Adsorption isotherms in ion exchange reactions. Further treatments and remarks on the application of the Langmuir isotherm. Colloids Surf. A. 1995; 97:129-140.

20. Nouri L, Ghodbane I, Hamdaoui O, Chiha M. Batch sorption dynamics and equilibrium of tri- and hexavalent chromium from water. J. Hazard. Mater. 2007;149:115-125.
21. Ahmaruzzaman M. Adsorption of phenolic compounds on low-cost adsorbents-a review. Adv. Colloid Interface Sci. 2008; 143:48-67.
22. Kalderis D, Koutoulakis D, Paraskeva P, Diamadopoulus E, Otal E, Del Valle JO, Pereira F. Adsorption of polluting substances on activated carbon prepared from rice husk and sugarcane bagasse. Chem. Eng. J. 2008;144:42-50.
23. Limousin G, Gaudet JP, Charlet L, Szenknect S, Barthes V, Krimissa M. Sorption isotherms: A review on physical bases, modeling and measurement. Appl. Geochem. 2007;22:249-275.
24. Umoren SA, Eduok UM, Oguzie EE. Corrosion inhibition of mild steel in 1M H_2SO_4 by polyvinyl pyrrolidine and synergistic iodide additives. Electrochim. Acta. 2008;26:533-546.
25. Obot IB, Obi-Egbedi NO. Fluconazole as an inhibitor for aluminium corrosion in 0.1 M HCl. Colloids Surf., A. 2008;230:207-212.
26. Amar H, Benzakour J, Derja A, Villemin D, Moreau B, Braisaz T. Piperidin-1-yl phosphonic acid and (4-phosphono-piperazin-1-yl) phosphoric acid: A new class of iron corrosion inhibitors in sodium chloride 3% media. Appl. Surf. Sci. 2006; 252:6162-6172.
27. Ituen EB, Akaranta O, James AO. 5-hydroxytryptophan: A novel eco-friendly corrosion and oilfield microbial inhibitor. 2015;SPE-178370-MS.
28. Saranya J, Sounthari P, Parameswari K, Chitra S. Acenaphtho[1,2]quinoxaline and acenaphtho[1,2] pyrazine s corrosion inhibitors for mild steel in acid medium. Measur. 2010;77:175-186.
29. Ige OO, Umoru LE. Effects of sheer stress on the corrosion behaviour of X-65 carbon steel: A combined mass-loss and profilometry study. Tribol. Int. 2016;94:155-164.
30. Solomon MM, Umoren SA. Insitu preparation, characterization and anti-corrosion property of polypropylene glycol/ silver nanoparticles composite for mild steel corrosion in acid solution. J. Colloids Interface Sci. 2016;462:29-41.
31. Mobin M, Rizvi M. Inhibitory effect of xanthan gum and synergistic surfactants additives for mild steel corrosion in 1M HCl. Carbohydr. Polym. 2016;136:384-393.
32. Bran C, Wang ZM, Han X, Chen C, Zhang J. Electrochemical response of mild steel in ferrous ion enriched and CO_2 saturated solutions. Corros. Sci. 2015;96:42-51.
33. Sangeetha Y, Meenakshi S, Sundaram CS. Interactions at the mild steel acid solution interface in the presence of o-fumaryl-chisotan: Electrochemical and surface studies. Carbohydr. Polym. 2016; 136:38-45.
34. Grassino AN, Halambek J, Djakovic S, RS. Brncic Dent. M., Grabaric Z. Utilization of tomato peel waste from canning factory as potential source of pectin production and application as tin corrosion inhibitor. Food Hydrocolloids. 2016;52:265-274.
35. Mala F, Yasakau KA, Carneiro J, Kallip S, Tedim J, Henriques T, Carbal A, Venancia J, Zheludkevic ML, Rerreira MGS. Corrosion protection of AA2024 by sol-gel coatings modified with MBT-traded polyuria micorcapsules. Chem. Eng. J. 2016;283:1108-1117.
36. Guo L, Zhu S, Zhang S. Experimental and theoretical studies of benzalkonium chloride as inhibitor for carbon steel corrosion in sulphuric acid. J. Ind. Eng. Chem. 2015;24:171-180.
37. Shaban SM, Aiad I, El-Sukkary MM, Soliman EA, El-Awady MY. Evaluation of some cationic surfactants based on dimethylaminopropyl amine as corrosion inhibitors. J. Ind. Eng. Chem. 2015;21: 1029-1038.
38. Ansari KR, Quraishi MA, Singh A. Pyridine derivatives as corrosion inhibitors for N80 steel in 15% HCl: Electrochemical, surface and quantum chemical studies. Measur. 2015;76:136-147.
39. Yadav M, Kumar S, Sinha RR, Bahadur I, Ebenso EE. New pyrimidine derivatives as efficient organic inhibitors for mild steel corrosion in acidic medium: Electrochemical, SEM, EDX, AFM and Surface studies. J. Mol. Liq. 2015;211:135-145.
40. Chaitra TK, Mohana KNS, Tandon HC. Thermodynamic, electrochemical and quantum chemical evaluation of some triazole Schiff bases as mild steel corrosion inhibitors in acid media. J. Mol. Liq. 2015;211:1026-1038.

41. Khadiri A, Saddik R, Bekkouche K, Anouniti A, Hammouti B, Benchat N, Bruachrine M, Solmaz R. Gravimetric, electrochemical and quantum studies of some pyridazine derivatives as corrosion inhibitors for mild steel in 1M HCl solution. J. Tai. Inst. Chem. Eng. 2015;000:1-13.
42. Zheng X, Zhang S, Li WM, Gong Yin L. Experimental and theoretical studies of 2-imidazolium-based ionic liquids as inhibitor for mild steel in sulphuric acid solution. Corros. Sci. 2015;95:168-179.
43. Verma C, Singh P, Bahadur I, Ebenso EE, Quraishi MA. electrochemical, thermodynamic, surface and theoretical investigation of 2-amino benzene-1,3-dicarbonitriles as green corrosion inhibitor for aluminium in 0.5 M NaOH. J. Mol. Liq. 2015;209:767-778.
44. Ngobiri NC, Oguzie EE, Oforka NC, Akaranta O. Comparative study in the inhibitive effect of sulfadoxine-pyrimethane and an industrial inhibitor on the corrosion of pipeline steel in petroleum pipeline water. Arab. J. Chem.
DOI: org/10.1016/j.arabjc.2015.04.004
45. Ansari KR, Quraishi MA. Effect of three component (aniline, formaldehyde and piperazine) polymer on mild steel corrosion in hydrochloric acid medium. J. Asso. Arab. Univ. Bas. Appl. Sci. 2015;8:12-18.
46. Zarrouk A, Hammouti B, Lakhlifi T, Trainsnel M, Vezin H, Bentiss F. New 1H-pyrole-2,5-dione derivatives as effective organic inhibitor of carbon steel corrosion in hydrochloric acid medium, electrochemical, XPS and DFT studies. Corros. Sci. 2015;90:575-584.
47. Barmatov E, Huges T, Nagl M. Efficiency of film-forming corrosion inhibitors in strong hydrochloric acid under laminar flow and turbulent flow. Corros. Sci. 2015;92:85-94.
48. Papavinasam S, Revie RW, Attard M, Demonz A, Michaelian K. Comparison of techniques for monitoring corrosion inhibitors in oil and gas pipelines. Corros. 2003;59:1096-1111.
49. Finsgar M, Jackson J. Application of corrosion inhibitors for steel in acidic media for the oil and gas industry: A review. Corros. Sci. 2014;86:17-41.
50. Massart DL, Vandeginste BGM, Buydens LMC, Jong SD, Lewi RI, Smeyers-Verbeke J. Handbook of Chemometrics and Qualimetrics A: Elsevier, Amsterdam; 1997.
51. Tasug G, Tuken T, Kircir N, Erbil M. Investigation of 2-aminoethanethiol as corrosion inhibitor for mild steel using response surface methodology (RSM). Ionics. 2014;20:287-294.
52. Shaban SM, Aiad I, El-Sukkary MM, Soliman EA, El-Awady MY. Inhibition of mild steel corrosion in acidic medium by vanillin cationic inhibitor. J. Mol. Liq. 2015; 203:26-28.
53. Hussin MA, Shah AM, Rehim AA, Ibrahim MNM, Perrin D, Brosse N. Antioxidant and anticorrosive properties of oil palm fron lignin extracted with different techniques. Ann. For. Sci. 2015;72:17-26.
54. Milosev I, Kovacevic N, Kovac J, Kokalj A. The roles of mercapto, benzene and methyl groups in the corrosion inhibition of imidazoles in copper: 1. Experimental and characterization. Corros. Sci. 2015;98:107-117.
55. Samide A, Tutunaru B, Jonescu C, Rotaru P, Simoiu L. Aminophylline: Thermal characterization and its inhibition properties for the carbon steel corrosion in acidic environment. J. Therm. Anal. Calorim. 2014;118:631-639.
56. Zhang J, Song Y, Su H, Zhang L, Cheng G, Zhao J. Investigation of Diosyros kaki leaf extracts as corrosion inhibitors and bactericide in oilfield. Chem. Cen. J. 2013; 7:109-114.
57. Fouda AS, Shalabi K, El-Awady GY, Merayyed HF. Chalcone derivatives as corrosion inhibitors for carbon steel in 1 M HCl solution. Int. J. Electrochem. Sci. 2014;9:7038-7058.
58. Geethanjali R, Subhashini S. Thermo-dynamic characterization of metal dissolution and adsorption of poly vinyl alcohol-grafted poly(acrylamidevinylsulfonate) on mild steel in hydrochloric acid. Electrochim. Acta. 2015;35-48.
59. Mert BD, Yuce AO, Kardas G, Yazici B. Inhibition effect of 2-amino-4-methylpyridine on mild steel corrosion: experimental and theoretical investigation. Corros. Sci. 2014;85:287-295.
60. Mourya P, Banerjee S, Singh MM. Corrosion inhibition of mild steel in acidic solution by *Targetes erecta* (marigold flower) extract as green inhibitor. Corros. Sci. 2014;85:352-363.

61. El-Haddad MN, Fouda AS. Electro-analytical, quantum and surface characterization studies on imidazole derivatives as corrosion inhibitors for aluminium in acidic media. J. Mol. Liq. 2015;209:480-486.
62. Kartsonakis LA, Stanciu S, Matei AA, Karaxi EK, Hristu R, Karantonis A, Charitidis CA. Evaluation of the protective ability of typical corrosion unhibitors for magnesium alloys towards Mg and ZK30 variant. Corros. Sci; 2015.
DOI: org/10.1016/j.corsci.2015.07.028
63. El-Meligi AA. Hydrogen production by aluminium corrosion in hydrochloric acid and using inhibitors to control hydrogen evolution. Int. J. Hydrogen Energy. 2011; 36:10600-10607.
64. Saolmaz R, Doner A, Kardas G. The stability of hydrogen evolution activity abd corrosion behaviour of Ni-Cu coatings with long term electrolysis in alkaline solution. Int. J. Hydrogen Energy. 2009;34:2089-2094.
65. Sanatkumar BS, Nayak J, Shetty AN. Influence of 2-(4-chlorophenyl)-2-oxoethylbenzoate on the hydrogen evolution and corrosion inhibition of 18Ni250 grade weld aged maraging steel in 1.0 M sulfuric acid medium. Int. J. Hydrogen Energy. 2012;37:9431-9442.
66. Flis-Kabulska I, Flis J. Hydrogen evolution and corrosion products on iron cathodes in hot alkaline media. Int. J. Hydrogen Energy. 2014;39:3597-3605.
67. Velimirovic M, Carnaito L, Schoups Q, Seuntjens P, Bastinens L. Corrosion rate estimation of microscale zerovalent iron particles via direct hydrogen production measurements. J. Harzad. Mater. 2014; 270:18-26.
68. Choudhry KI, Carvajal-Ortiz RA, Kallikragas DT, Svischer IM. Hydrogen evolution rate during the corrosion of stainless steel in supercritical water. Corros. Sci. 2014;83:226-233.
69. Deyab MA. Effects of halide ions on hydrogen production during aluminium corrosion in formic acid and using some inorganic inhibitors to control hydrogen evolution. J. Power Sources. 2013;242:86-90.
70. Heakal FE, Tantawy NS, Shehata OS. Influence of Cerium (ii) ions on corrosion and hydrogen evolution of carbon steel in acidic solutions. Int. J. Hydrogen Energy. 2012;37:19219-19230.
71. Wu L, He Y, Lei T, Nan B, Xu N, Zou J, Huang B, Liu CT. The stability of hydrogen evolution activity and corrosion behaviour of porous NyAl-Mo electrode in alkaline solution during long term electrolysis. Energy. 2014;67:19-26.
72. Thomas S, Medhekar NV, Frankel GS, Birbilis N. Corrosion mechanism and hydrohen evolution on Magnessium. Curr. Opin. Solid State Mater. Sci. DOI: 10.1016/j.cossms.2014.09.005
73. Curioni M, Scenini F, Monetta T, Bellulai F. Correlation between electrochemical impedance measurement and corrosion rate of magnesium investigated by real-time hydrogen measurement and optical imaging. Electrochim. Acta. 2015;160:372-384.
74. Curoinin M. The behaviour of magnesium during free corrosion and potentiodynamic polarization investigated by real-time hydrogen measurement and optical imaging. Electrochim. Act. 2014;120:284-292.
75. Kalaiselvi K, Nijarubini V, Mallika J. Investigation of the inhibitive effects of 1,8-naphthylidine derivatives on corrosion of mild steel in acidic media. J. Chem. 2013;6:52-64.
76. Abbound Y, Hammouti B, Abbourriche A, Ihasane B, Bennamara A, Charrouf M, Al-Deyab SS. 2-(o-hydroxyphenyl) benzimidazole as a new corrosion inhibitor for mild steel in hydrochloric acid solution. Int. J. Electrochem. Sci. 2012;7:2543-2551.
77. Umoren SA, Eduok UM, Solomon MM, Udoh AP. Corrosion inhibition by leaves and stem extracts of *Sida acuta* for mild steel in 1M H_2SO_4 solutions investigated by chemical nd spectroscopic techniques. Arab. J. Chem; 2011.
DOI: 10/1016/j.arabjc.2011.03.008
78. Ayyasamy K, Palanisamy S, Kandasamy P, Chitra S. Polyester-bentonite clay composite: Synthesis, characterization and application as anticorrosive agent. Oreintal J. Chem. 2015;31:1811-1821.
79. Ali OAM. Palladium (ii) and Zinc (ii) complexes of neutral $[N_2O_2]$ donor Schiff basas derived from fufuraldehyde: synthesis, characterization, fluorescence and corrosion inhibition of ligands. Spectrochim Acta, A. 2014;132:52-60.
80. Singh AK, Shukla Singh M, Quraishi MA. Inhibitive effect of ceftazidine on corrosion

of mild steel in hydrochloric acid solution. Mater. Chem. Phy. 2011;129:68-76.
81. Vadi M, Abbasi M, Zakeri M, Yazdi J. Application of the Freundlich, Langmuir, Temkin and Harkins-Jura adsorption isotherms for some amino acida and amino acdis complexation with manganese (ii) on carbon nanotube. Proceedings of International Conference of Nanotechnology and Biosensors; 2010.
82. Finsgar M. 2-mercaptobenzimidazole as a copper corrosion inhibitor: Part 1. Long term immersion, 3D-profilometry, and electrochemistry. Corros. Sci. 2013;72:82-89.
83. El-Sukkary M, Kertit M, Guottaya HM, Nciri B, Ben Souda Y, Perez I, Infante MR, Elkacemi K. The preparation and characterization of some noven quaternary iminium salts based on schiff base as corrosion inhibitor. Petrol. Sci. Technol. 2005;28:1158-1164.
84. Migahed MA, Attya MM, Rashwan SM, El-Raouf MA, Al-Sabagh AM. Synthesis of some novel non-ionic surfactants based on tolyltriazole and evaluation of their performances as corrosion inhibitors for carbon steel. Egypt. J. Petrol. 2013; 22:149-160.
85. Tian H, Cheng YF, Li W, Hou B. Triazodyl-acylhydrazone derivatives as novel corrosion inhibitor for copper corrosion in chloride solutions. Corros. Sci. DOI: org/10.1016/j.corsci.2015.08.022
86. OZa BN, Sinha RS. Thermometric study of corrosion behaviour of high strength Al-Mg alloy in phosphoric acid in presence of halides. Tanstact. Saest. 1982;17/4:281-285.
87. Batsida DM, Gomez PP, Cano E. The isotherm shape, a criterion for studying the adsorption mechanism of benzotriazole on copper in sulphuric acid Rev. Metall. 2005; 41:98-106.
88. Eddy NO, Ebenso EE. Adsorption and inhibitive property of ethanol extract of Musa sapientun peels as a green corrosion inhibitor for mild steel in H_2SO_4. Afri. J. Pur. Appl. Chem. 2008;2:046-054.
89. Martinez S, Stern I. Thermodynamic characterization of metal dissolution and inhibitor adsorption process in low carbon steel/mimosa tannin/sunfuric acid system. Appl. Surf. Sci. 2002;199:83-89.
90. Valek K, Martinez S. Copper corrosion inhibition by *Azidirachta indica* leaves extract in 0.5 M sulfuric acid. Mater. Lett. 2007;61:148-151.
91. Abd El-Rehim SS, Hassan HH, Amin MA. Corrosion study of pure aluminium and some of its alloys in 1.0 M HCl solution by impedance technique. Electrochim. Act. 2008;26:267-282.
92. Umoren SA, Obot IB, Ebenso EE, Okafor PC. Eco-friendly inhibitors from naturally occurring exudate gums for aluminium corrosion inhibition in acidic medium. Electrochim. Act. 2008;26:267-282.
93. Fouda AS, Ellithy AS. Inhibition effect of 4-phenylthiazolederivatives on corrosion of 304L Stainless steel in HCl solution. Corros. Sci. 2009;51:868-875.
94. Adejo SO, Ekwenchi MM, Gbertyo JA, Ogbodo JO. Determination of adsorption isotherm model best fit for methanol extract of *Securinega virosa* as corrosion inhibitor for corrosion of mild steel in HCl. J. Adv. Chem. 2014;10:2737-2742.
95. Bouklah M, Hammouti B, Lagrenee M, Bentiss F. Thermodynamic properties of 2,5-bis(4-methylphenyl)-1,3,4-oxadiazole as a corrosion inhibitor for mild steel in normal sulfuric acid medium. Corros. Sci. 2006;48:2831-2842.
96. Bentiss F, Lebrini M, Lagrenee M. Thermodynamic characterization of metal dissolution and inhibitor adsorption process in mild steel/2,5-bis(methyl)-1,3,4-thiadazoles/hydrochloric acid medium. Corros. Sci. 2005;47:2915-2931.
97. Chanovska D, Cvetkovska M, Grchev T. Corrosion inhibition of iron in hydrochloric acid by polyacrylamide. J. Serb. Chem. Soc. 2007;72:687-698.
98. Sharma SK, Mudhor A, Jain G, Sharma J. Corrosion inhibition and adsorptive properties of *Azadirachta indica* mature leaves extract as green inhibitor for mild steel in HNO_3. Green Chem. Lett. Rev. 2010;3:17-25.
99. Abbasov VM, El-Lateef HM, Aliyera LI, Qasimov EE, Ismayilov IT, Khalaf MM. A study of corrosion inhibition of mild steel C1018 in CO_2-saturated brine using some novel surfactants based on corn oil. Egypt. J. Petrol. 2013;22:451-470.
100. Paul S, Kar B. Mitigation of mild steel corrosion in acid by green inhibitors: Yeast, pepper, garlic and coffee. ISRN Corros. DOI: 5402/2012/641386
101. Badr GE. The role of some thiosemicarbozide derivatives as corrosion

inhibitors for carbon steel in acidic media. Corros. Sci. 2009;51:2529-2536.
102. El-Awady GY, El-Said IA, Fouda AS. Anion surfactants as corrosion inhibitors for aluminium dissolution in HCl solutions. Int. J. Electrochem. Sci. 2008;3:174-190.
103. Oguzie EE. Corrosion inhibition of aluminium in acidic and alkaline media by *Sansevieria trifasciata* extract. Corros. Sci. 2007;49:1527-1539.
104. El-Sherif RM, Badawy WA. Mechanism of corrosion and corrosion inhibition of tin in aqueous solution containing tartaric acid. Int. J. Electrochem. Sci. 2011;6:6469-6482.
105. Verma C, Singh P, Quraishi MA. A thermodynamic, electrochemical and surface investigation of Bis(indolyl) methanes as green corrosion inhibitors for mild steel in 1M HCl acid solution. J. Asso. Arab Univ. Bas. Appl. Sci; 2016.
DOI: 10'1016/j.jaubas.2015.04.003
106. Noor EA. Temperature effects on the corrosion inhibition of mild steel in acidic solution by aqueous extracts of Fenugreek leaves. Inter. J. Electrochem. Sci. 2007; 2:996-1017.
107. Tang L, Mu G, Liu G. The effects of neutral red on the corrosion inhibition of cold rolled steel in 1.0 M hydrochloric acid. Corros. Sci. 2003;45:2251-2262.
108. Arsian T, Kandemirli F, Ebenso EE, Love L, Alemu H. Quantum chemical studies on the corrosion inhibition of some sulphonamides on mild steel in acidic medium. Corros. Sci. 2009;5:35-47.
109. Larabi L, Harek Y, Traisnel M, Mansri A. Synergistic influence of poly 94-vinylpyridine) and potassium iodide on inhibition of corrosion of mild steel in 1M HCl. J. Appl. Electrochem. 2014;34:833-839.
110. Ebenso EE. Synergistic effect of halide ions on the corrosion inhibition of aluminium in H_2SO_4 using 2-acetylphenothiazine. Mater. Chem. Phys. 2003;79:58-70.
111. Ituen EB, Udo UE, Odozi NW, Dan EU. Adsorption and kinetic/thermodynamic characterization of aluminium corrosion in sulphuric acid by extract of *Alatonia boonei*. J. Appl. Chem. 2013;3:52-59.
112. Ituen EB, Essien EA, Udo UE, Oluwaseyi OR. Experimental and theoretical study of effect of *Cucumeropsis manni* N. seed oil metallic soap of zinc on mild steel surface in sulphuric acid. Adv. Appl. Sci. 2014;5: 26-53.
113. Bhat JI, Alva VOP. Inhibition effect of Navirapine an antiretroviral on the corrosion of mild steel under acidic condition. J. Korean Chem. Soc. 2011;55: 835-841.
114. Oguzie EE, Okolue BN, Ebenso EE, Onuoha GN, Onuchukwu AI. Evaluation of inhibitory effect of methylene blue dye on corrosion of aluminium in HCl. Mater. Chem Phys. 2004;87:394-401.
115. Yurt A, Ulutas S, Dal H. Electrochemical and theoretical investigation on the corrosion of aluminum in acidic solution containing some Schiff bases. Appl. Surf. Sci. 2005;253:919-925.
116. Villamil RFV, Corio P, Rubim JC, Agostinho SML. Effect of sodium dodecylsulphate on copper corrosion in sulphuric acid media in the absence and presence of benzotriazole. J. Electroanal. Chem. 1999;47:112-117.
117. Ikpi ME, Udoh II, Okafor PC, Ekpe UJ, Ebenso EE. Corrosion inhibition and adsorption behaviour of extract of *Piper guineensis* on mild steel corrosion in acidic media. Int. J. Electrochem. Sci. 2012;7: 12193-12206.
118. Obot IB, Umoren SA, Obi-Egbedi NO. Corrosion inhibition and adsorption behaviour of aluminium by extracts of *Amingeria rubusta* in HCl solution: Synergistic effects of halide ions. J. Mater. Environ. Sci. 1022;2:60-71.
119. Yuce AO, Solmaz R, Kardas G. Investigation of inhibition effect of rhodamine-N-acetic acid on mild steel corrosion in HCl solution. Mater. Chem. Phys. 2012;131:615-620.
120. Obi-Egbedi NO, Obot IB, Eseola EA. Synthesis, characterization and corrosion inhibition efficiency of 2-(6-methylpyridinyl-1H-imidazo[4,5-f][1,10]phenanthroline on mild steel in sulphuric acid. Arab. J. Chem. 2014;7:197-207.
121. Szlarska-smialowska Z, Mankowski J. Crevice corrosion of stainless steels in sodium chloride solution. Corros. Sci. 1978;18:953-960.
122. Obi-Egbedi NO, Obot IB. Xanthione: A new and effective corrosion inhibitor for mild steel in sulphuric acid solution. Arab. J. Chem. 2011;6:211-223.
123. Hu Q, Zhang G, Qiu Y, Guo X. The crevice corrosion behaviour of stainless steel in

sodium chloride solution. Corros. Sci. 2010;53:4065-4072.
124. Abd El-Lateef HM, Abbasov IM, Aliyeva LI, Khalaf MM. Novel naphthenate surfactants based on petroleum acids and nitrogeneous bases as corrosion inhibitors for C1018 type mild steel in CO_2-saturated brine. Egypt. J. Petrol. 2015;24:175-182.
125. Kern P, Landlort O. Adsorption of our organic corrosion inhibitor on iron and gold studied with a rotated EQCM. J. Electrochem. Soc. 2001;48:8228-8235.
126. Abdullah A. Adsorption isotherms of some triazoles as corrosion inhibitor of mild steel in acids. Al-Fatih. 2008;32:1-10.
127. Obot IB, Obi-Egbedi NO. Ginseng roots: A new efficient and effective ecofriendly corrosion inhibitor for aluminium alloy of type AA1060 in hydrochloric acid solution. Inter. J. Electrochem. Sci. 2009;4:1277-1288.
128. Orlanacic H, Stupnisek-Lisac B, Copper corrosion inhibition in near neutral media. Portug. Electrochim. Act. 2003;48:985-991.
129. Obot IB, Obi-Egbedi NO, Umoren SA. The synergistic inhibitive effect and some quantum chemical parameters of 2,3-diaminonaphthalene and iodide ion in hydrochloric acid corrosion of aluminium. Corros. Sci. 2009;51:276-282.
130. Eduok UM, Umoren SA, Udoh AP. Synergistic inhibition effect between leaves and stem extracts of *Sida acuta* and iodine ion for mild steel corrosion in 1M H_2SO_4 solution. J. Chem. 2012;5:325-337.
131. El-Rabiee MM, Helal NH, Abd El-Hafet GM, Badawy WA. Corrosion control of vanadium in aqueous solutiions by amino acids. J. Alloy. Comp. 2008;459:466-471.
132. Seifzadeh D, Basharnawaz H, Bezaatpour A. A Schiff base compound as effective corrosion inhibitor for magnesium in acidic media. Mater. Chem. Phys. 2013'138:794-802.
133. Dada AO, Olalekan AP, Olatunya AP, Dada O. Langmuir, Freundlich, Temkin and Dubinin-Raushkevich isotherms studies of equilibrium sorption of zinc (ii) ions onto pphosphoric acid modified rice husk. J. Appl. Chem. 2012;3:38-45.
134. Webber TN, Chakravarti RK. Pore solid diffusion models for fixed bed adsorbers. J. Amer. Inst. Chem. Eng. 1974;20:228-238.
135. Khadom AA, Yaro AS, Khadum AAH. Adsorption mechanism of benzothiazole for corrosion inhibition of copper-nickel alloy in hydrochloric acid. J. Chilean Chem. Soc. 2010;55:150-152.
136. Oguzie EE, Unaegbu C, Ogukwe CN, Okolue BN, Onochukwu AI. Inhibition of mild steel corrosion in sulfuric acid using indigo dye and synergistic halide additives. Mater. Chem. Phys. 2004;84:363-368.
137. Martinez S. Inhibitory mechanism of momosa tannin using molecular modeling and substitutional adsorption isotherms. Mater. Chem. Phys. 2002;77:97-102.
138. Abdel-Gaber AM, Abd El-Nabey SA, Sidahmed IM, El-Zayady AM, Saadawy M. Inhibitive action of some plant extracts on corrosion of steel in acidic media. Corros. Sci. 2006;48:2765-2779.
139. Umoren SA, Ebenso EE. Synergistic effect of polyacrylamide and iodide ions on the corrosion inhibition of mild steel in H_2SO_4. Mater. Chem. Phys. 2007;106:387-393.
140. Saratha R, Priya SV, Thilagavanthy P. Investigation of *Citrus aurantifolia* leaves extract as corrosion inhibitor for mild steel in 1 M HCl. E-Jour. Chem. 2009;6:785-795.
141. Deyap MA. Effects of cationic surfactant and inorganic ions on the electrochemical behaviour of carbon steel in formation water. Corros. Sci. 2007;49:2315-2328.
142. Abd El-Rehim SS, Ibrahim MAM, Khalia KE. The inhibiton of 4-2I-amino-5-methyl phenylazo)antipyrine on corrosion of mild steel in HCl solution. Mater. Chem. Phys. 2001;70:268-273.
143. Oguzie EE. Influence of halide ions on the inhibitive effects of congo red dye on the corrosion of mild steel in sulfuric acid medium. Mater. Chem. Phys. 2004;87:212-217.
144. Li Y, Zhao P, Liang Q, Hou B. Berberine as a natural source inhibitor for mild steel in 1 M H_2SO_4. Appl. Surf. Sci. 2005;252:1245-1253.
145. Eddy NO, Ebenso EE. Adsorption and inhibitive property of ethanol extract of *Musa sapientun* peels as a green corrosion inhibitor for mild steel in H_2SO_4. Afri. J. Pur. Appl. Chem. 2008;2:046-054.
146. Fouda AS, Al-Sarawy AA, El-Katori EE. Pyrazolone derivatives as corrosion inhibitors for carbon steel in hydrochloric acid solution. Desall. 2006;201:1-13.
147. Abd El-Rehim SS, Hassan HH, Amin MA. Corrosion inhibition by 1,1(laurylamido) propyl ammonium chloride in HCl solution. Mater. Chem. Phys. 2001;70:64-72.

148. De Souza FS, Spinelli A. Cffeic acid as a green corrosion inhibitor for mild steel. Corros. Sci. 2009;51:64-72.
149. Vracar DLM, Drazic M. Adsorption and corrosion inhibitive properties od some organic molecules on iron electrode in sulphuric acid. Corros. Sci. 2002;44:1669-1680.
150. Abd El-Rehim SS, Hassan HH, Amin MA. The corrosion inhibition study of sodium dodecybenzene sulphonate for aluminium and its alloys in 1 M HCl solution. Mater. Chem. Phys. 2002;78:337-348.
151. Abd El-Rehim SS, Hassan HH, Amin MA. Corrosion inhibition study of pure aluminium and some of its alloys in 1.0 M HCl solution by impedance technique. Corros. Sci. 2004;46:2-25.
152. Batidas JM, Oinilla P, Cano E, Polo JL, Miguel S. Copper corrosion inhibition by triphenylmethane derivatives in sulphuric acid media. Corros. Sci. 2003;45:427-449.
153. Nataraja SE, Venkatesha TV, Majunatha Poojary B, Pavithra MK, Tandon HC. Inhibition of corrosion of steel in hydrochloric acid solution by some organic molecules containing the methylthiophenyl moiety. Corros. Sci. 2011;53:2651-2659.
154. Sahin M, Bilgic S, Yalmaz H. The inhibition effects of some cyclic nitrogen compounds on the corrosion of thee mild steel in NaCl mediums. Appl. Surf. Sci. 2002;195:1-7.
155. Durnie W, De Marco R, Jefferson A, Kinsella B. Development of a structur-activity relationship for oilfield corrosion inhibitors. J. Electrochem. Soc. 2002;146: 1751-1756.
156. Hossani M, Mertens SFL, Ghorbani M, Arshadi MR. Assymetrical schiff bases as inhibitors of mild steel corrosion in sulphuric acid medium. Mater. Chem. Phys. 2003;78:800-808.
157. Moussa MNH, El-Far AA, El-Shafei AA. The use of water soluble hydrazones as inhibitor for the corrosion of carbon steel in acidic medium. Mater. Chem. Phy. 2008; 105:105-113.
158. Al-Andis N, Khamis E, Al-Mayouf A, Aboul-Enein H. The kinetics of steel dissolution in the presence of some thiouracil derivatives. Corros. Prev. Cont. 1995;42: 13-18.
159. Foad EE, Abdel Wahaab IM, Deyab M. Exothylated fatty acids as corrosion inhibitors for the corrosion of zinc in cid media. Chem. Phys. 2005;89:183-191.
160. El-Shafei AA, Moussa MHN, El-Far AA. The corrosion inhibition character of thiosemicarbazide and its derivatives for carbon steel in hydrochloric acid solution. Mater. Chem. Phys. 2001;70:175-180.
161. Foad EE. Sulphamethoxazole as an effective inhibitor for the corrosion of mild steel in 1.0 M HCl solution. Mater. Chem. Phys. 1999;61:223-228.
162. Umoren SA, Obot IB, Ebenso EE, Obi-Egbedi NO. Inhibition of aluminium corrosion in hydrochloric acid solution by exudate gum from *Raphia hookeri*. Desall. 2009;247:561-572.
163. Umoren SA, Li Y, Wang FH. (Electrochemical study of corrosion inhibition and adsorption behaviour of pure iron by polyacrylamide in H2SO4-Synergistic effect of iodide ions. Corros. Sci. 2010;52:1777-1786.
164. Lukovits I, Kalman E, Palinkas G. Non-linear group contribution models of corrosion inhibition. Corros. 1995;51:201-205.
165. Subramanyam NC, Shshadri BS, Mayanna SM. Thiourea and substituted thioureas as corrosion inhibitor for aluminium in sodium nitrite solution. Corros. Sci. 1993;34:563-571.
166. Guartarone G, Moretti G, Bellomi T, Capobianco G, Zingales A. Using indole to inhibit copper corrosion in aerated 0.5 M H_2SO_4 acid. Corros. 1998;54:606-618.
167. Bouyanzer A, Hammouti B. A study of corrosive effect of artemisia oil on steel. Pig. Res. Technol. 2004;33:287-292.
168. Umoren SA, Obot IB. Polypyrollidone and polyacrylamide as corrosion inhibitor for mild steel in acidic medium. Surf. Rev. Lett. 2008;15:287-292.
169. Gasparac R, Martin CR. S. Isaac. Insitu studies of imidazoles and its derivatives as copper corrosion inhibitors. I. Activation energies and thermodynamics of adsorption. J. Electrochem. Soc. 2000; 144:548-551.
170. Singh AK, Quraishi MA. Investigation of the effect of disulfram on corrosion of mild steel in hydrochloric acid solution. Corros. Sci. 2011;53:1288-1297.
171. Singh AK, Shukla IK, Singh M, Quraishi MA. Inhibition effect of ceftazidime on corrosion of mild steel in hydrochloric acid solution, Mater. Chem. Phys. 2011;129:68-76.
172. Belayachi M, Zarrik H, El-Assyry A, Zarrouk A, Ouda H, Boukhris S, Hammouti

B, Ebenso EE, Geunbour A. New pyrimidothiazine derivative as a corrosion inhibitor for carbon steel in acidic media. Int. J. Electrochem. Sci. 2015;10:3010-3025.
173. Hussin MH, Rabim AA, Ibrahim MNM, Brosse N. Improved corrosion inhibition of mild steel by electrochemically modified lignin polymers from *Elaeis guineensis* agricultural waste. Mater. Chem Phys. 2015;163:210-212.
174. Mistry BM, Sahw SK, Kim DH, Jauhari S. Tetrazoleo[1,5-a]quinolone-4-carbaldehyde and its Schiff base on mild steel as corrosion inhibitor in 1M HCl solution: Electrochemistry, theoretical and SEM surface analysis. Surf. Interface Anal. 2015;47:706-718.
175. Deyab MA. Corrosion inhibition of aluminium in biodiesel by extracts of Rosemary leaves. J. Tai. Inst. Chem. Eng. 2015;000:706-718.
176. Quraishi MA, Jamal D. Fatty acid triazoles: Novel corrosion inhibitors for oil well steel (N80) and mild steel. JAOCS. 2000;77: 1107-1111.
177. Quraishi M, Jamal D. Corrosion inhibition of N-80 steel and mild steel in 15% boiling hydrochloric acid by triazole component-SAHMT. Mater. Chem. Phys. 2001;68:283-287.
178. Neha P, Diva L, Nisha S. Inhibition effect of *Hibiscus rosa sinessiis* leaves extract on corrosion of mild steel in HCl medium. Int. J. Resear. Chem. Environ. 2015;5:33-41.
179. El-Hamdani N, Fdil R, Tourabi M, Jama C, Bentiss F. Alkaloids extract of *Retama monosperma* (L) bioss seeds used as novel ecofriendly inhibitor for carbon steel corrosion in 1 M HCl solution: Electrochemical and surface studies. Appl. Surf. Sci. 2015;357:1294-1305.
DOI: 10.1016/j.apsusc.2015.09.159
180. Abd El-Lateef HM, Abu-Dief AM, Abdel-Rahman LH, Sanudo EC, Aliaga-Alcalde N. Electrochemical and theoretical quantum approach on the inhibition of C1018 steel corrosion in acidic medium containing chloride using some newly synthesized phenolic Schiff bases compounds. J. Electroanal. Chem. 2015; 743:120-133.
181. Saha SK, Dutta A, Gihosh P, Sukul D, Banerjee P. Adsorption and corrosion inhibition effect of Schiff base molecules on the mild steel surface in 1 M HCl solution: A combined experimental and theoretical approach. Phys. Chem. Chem. Phys. 2015;17:5679-5690.
182. Ansari KR, Quraishi MA. Experimental and quantum chemical investigation of Schiff bases of isatin as new and green corrosion inhibitors of mild steel in 20% H_2SO_4. J. Tai. Inst. Chem. Eng. 2015;54:145-154.
183. Verma CB, Ebenso EE, Bahadur I, Obot I B, Quraishi MA. 5-(phenylthio)-3H-pyrrole-4-carbonitriles as effective corrosion inhibitors for mild steel in HCl. Experimental and theoretical investigation. J. Mol. Liq. 2015;212:209-218.
184. Olvera-Martinez ME, Mendoza-Flores J, Genesca J. Carbondioxide corrosion control in steel pipelines influence of turbulent flow on performance of corrosion inhibitors. J. Loss Prev. Proc. Ind. 2015; 35:19-28.
185. Rames-Kumar S, Danaee I, RashvandAvei M, Vijayan M. Quantum chemical and experimental investigations of equipotent effect of (+)R and (-)S enantiomers of racemic anisulprides as eco-friendly corrosion inhibitors for ild steel in acidic solution. J. Mol. Liq. 2015;212:168-186.
186. Yurt A, Duran B, Dal H. An experimental and theoretical investigation on adsorption properties of some diphenolic Schiff bases as corrosion inhibitors at acid/mild steel interface. Arab. J. Chem. 2014;7:732-740.
187. Shihab MS, Al-Doori HH. Experimental and theoretical study of N-substituted p-aminoazobenzene derivatives as corrosion inhibitors for mild steel in sulphuric acid solution. J. Mol. Liq. 2014;1076:658-663.
188. Khadon AA, Hassan AF, Abod BM. Evaluation of environmentally friendly inhibitor for galvanic corrosion of steel-couple in petroleum waste water. Process Saf. Environ. Prot. 2015;98:93-101.
189. Sabagh AM, Kandile NG, Nasser NM, Mishrof MR. Tabey AE. Novel surfactants incorporated with 1,3,5-triethanolhexahydro-1,3,5-triazine moiety as corrosion inhibitor for carbon steel in hydrochloric acid: Electrochemical and quantum chemical investigations. Egypt. J. Petrol. 2015;22:351-365.
190. Zhang HH, Pang X, Zhou M, Liu C, Wei L, Gao K. The behaviour of pre-corrosion effect on the performance of imidazoline-based inhibitor in 3wt% NaCl solution saturated with CO2. Appl. Suf. Sci. 2015; 356:63-72.
191. Odewunmi NA, Umoren SA, Gasem ZM. Watermelon waste products as green

corrosion inhibitors for mild steel in HCl solutions. J. Environ. Chem. Eng. 2015;3: 286-296.
192. Shabani-Nooshabadi M, Ghandehi MS. Santolina chamaecyprissus extract as a natural source inhibitor for 304 stainless steel corrosion in 3.5% NaCl. J. Indus. Eng. Chem. 2015;31:231-237.
193. Singh A, Lin Y, Obot IB,. Ebenso EE,. Ansari KR, Quraishi MA. Corrosion mitigation of J55 steel in 3.5% NaCl solution by a macrocyclic inhibitor. Appl. Surf. Sci. 2015;356:341-347.
194. Noor El-Din MR, Khamis EA. Utilization of sulfidated poly(acrylvinylacetate) as a new corrosion inhibitor for carbon steel in acidic media. J. Indus. Eng. Chem. 2015;24:342-350.
195. Zhang K, Xu B, Yang W, Yin X, Liu Y, Chen Y. Halogen substituted imidazoline derivatives as corrosion inhibitors for mild steel in hydrochloric acid solution, Corros. Sci. 2015;90:284-2965.
196. Hamani H, Douadi T, Al-Noaimi M, Issaadi S, Daoud D, Chafaa S. Electrochemical and quantum chemical studies of some azomethane compounds as corrosion inhibitors for mild steel in 1M hydrochloric acid. Corros. Sci. 2014;88:234-245.
197. Bhawsar J, Jain PK, Jain P. Experimental and computational studies of *Nicotiana tabacum* leaves extract as green corrosion inhibitor for mild steel in acidic medium. Alexan. Eng. J. 2015;54:769-775.
198. Lazano I, Mazario E, Olivares-Xometi CO, Likhanova NV, Herrasti P. Corrosion behaviour of API-5LX52 steel in HCl and H_2SO_4 media in the presence of 1,3-dibencilimidazolio acetate and 1,3-dibencilimidazolio dodecanoate ionic liquids as corrosion inhibitors. Mater. Chem. Phys. 2014;147:191-197.
199. Mazumber MAJ, Al-Mulallem HA, Faiz M, Ali SA. Design and synthesis of a novel class of inhibitors for mild steel corrosion in acidic and carbondioxide-saturated saline media. Corros. Sci. 2014;87:187-198.
200. Hejazi S, Mohajerrzia S, Moayed MH, Davoodi A, Rahimizadeh M, Momeni M, Elsami A, Shiri A, Kosari A. Electrochemical and quantum chemical study of thiazolo-pyrimidine derivatives as corrosion inhibitors on mild steel in 1 M H_2SO_4. J. Ind. Eng. Chem. 2015;25:112-121.
201. Yadav M, Kumar S, Tiwari I, Bahadur I, Ebenso EE. Experimental and quantum chemical studies of synthesized triazine derivatives as an efficient corrosion inhibitor for n80 steel. J. Mol. Liq. 2015; 212:151-167.
202. Hegazy MA, Aiad I. 1-dodecyl-4-(((3-morpholinopropyl)iminomethyl)pyridine-1-ium) bromide as a novel corrosion inhibitor for carbon steel during phosphoric acid production. J. Ind. Eng. Chem. 2015;31:91-99.
203. Ituen EB, Akaranta O, James AO. Green anticorrosive oilfield chemicals from seeds and leave eextracts of *Griffonia simplicifolia* for mild stel. J. Chem. Mater. Res. 2016;5:45-57.
204. Hu Q, Qui Y, Zhang G, Guo X. *Capsella bursa-pastoris* extract as eco-friendly inhibitor on the corrosion of Q235 carbon steel in 1molL-1 hydrochloric acid. Chin. J. Chem. Eng. 2015;23:1408-1415.
205. Biswas A, Pal S, Udayahbanu G. Experimental and theoretical studies on xanthan gum and its grant copolymer as corrosion inhibitor for mild steel in 15% HCl. Appl. Surf. Sci. 2015;353:173-183.
206. Golestani G, Shahidi M, Ghazanfari D. Experimental evaluation of antibacterial drugs as environment-friendly inhibitors for corrosion of carbon steel in HCl solution. Appl. Surf. Sci. 2014;308:347-362.
207. Eddy NO, Momoh-Yahaya H, Oguzie EE. Theoretical and experimental studies on the corrosion inhibition potential of some purines for aluminium in 0.1 M HCl. J. Adv. Resear. 2015;6:203-217.
208. Hong S, Chen W, Luo HQ, Li NB. Inhibitive effect of 4-mainoantipyrine on the corrosion of copper in 3wt.% NaCl. Corros. Sci. 2012;57:270-278.
209. Okeniyi JO. $C_{10}H_8N_2Na_2O_{10}$ inhibition and adsorption mechanism on concrete-reinforcement corrosion in corrosive environments. J. Asso. Arab. Univ. Bas. Appl. Sci; 2016.
DOI: org/10.1016/j.jaubas.2014.08.004
210. Abdel-Gaber AM, Khalil MS, Sheheta EE. Electrochemical study on the effect of Schiff base and its cobalt complex on the acid corrosion of steel. Corros. Sci. 2009; 51:3021-3024.
211. Olivares O, Likhanova NV, Gomez B, Navarrete J, Llanos-Serrano ME, Arce E, Hallen JM. Electrochemical and XPS studies on decylamides of aminoacids adsorption on carbon steel in acidic environment. Appl. Surf. Sci. 2006;252: 2894-2909.

212. Algabar AS, El-Nemma EM, Saleh MM. Effect of octylphenolpolyethylene oxide on the corrosion inhibition of steel in 0.5 M H_2SO_4. Mater. Chem Phys. 2004;86:26-32.
213. Oguzie EE, Li Y, Wang FH. Corrosion inhibition and adsorption behaviour of methionine on mild steel in sulphuric acid and synergistic effect of iodide ion. J. Colloid Interface Sci. 2007;310:90-98.
214. Bouyanzer A, Hammouti B, Majidi L. Pennyroyal oil from *Mentha pulegium* as corrosion inhibitor for steel in 1.0 M HCl. Mater. Lett. 2007;60:2840-2843.
215. Obot IB, Obi-Egbedi NO. Adsorption properties and inhibition of mild steel corrosion in sulphuric acid solution by ketoconazole: Experimental and theoretical investigation. Corros. Sci. 2010;52:198-204.
216. Foad El-Sherbini EE, Abd El-Wahab, Deyab MA. Studies on corrosion inhibition of aluminium in 1.0 M HCl and 1.0 M H_2SO_4 solutions by ethoxylated fatty acids. Mater. Chem. Phys. 2003;82:631-637.
217. Keera ST, Deyab MA. Effect of some organic surfactants on the electrochemical behaviour of carbon steel in formation water. Colloids Surf. 2005;266:129-140.
218. Fouda AS, Al-Sarawy AA, Ahmed FS, El-Abbasi HM. Corrosion inhibition of aluminium 6063 using some pharmaceutical compounds. Corros. Sci. 2009;51:485-492.
219. Obot IB. Synergistic effects of Nizoral and iodide ions on the corrosion inhibition of mild steel in sulphuric acid solution. Electrochim. Act. 2009;27:539-553.

Peer-review history:
The peer review history for this paper can be accessed here:
http://sciencedomain.org/review-history/17611